FINGER KNUCKLES PATTERNS AND FINGERNAILS RECOGNITION FOR PERSONAL IDENTIFICATION BASED ON MULTI-MODEL DEEP LEARNING FEATURES

Haitham Salman Chyad[1*] and Tarek Abbes[2]

[1*,2] NTS'COM, National School of Electronics and Telecommunications of Sfax, University of Sfax, Tunisia

Emails: dr.haitham@uomustansiriyah.edu.iq[1*] (Corresponding Author), tarek.abbes@enetcom.usf.tn[2]

ABSTRACT

Because biometric recognition systems are reliable and distinctive, they are widely used in many different applications. Hand-based person recognition has gained a lot of attention in recent years because of its stability, feature richness, dependability, and increased user acceptance. Although the dorsal side of the hand can be quite helpful in personal identification, it does not receive much attention. Finger knuckle and finger nail biometric traits can be obtained from a single dorsal hand scan. This research paper presents an approach for person identification using the dorsal finger knuckle and fingernails. It provides a structure for automatic person identification, which includes the segmentation of the detected components with hand images using the Hands Module (Media Pipe Module). The research paper focuses on the key points that hand components consist of the base knuckle, the major knuckle, the minor knuckle, the thumb knuckle, and the fingernails, which are one of the important biometric features. Specifically, a multi-model deep learning neural network (DLNN) is used to extract distinct features from each model using the DenseNet201 and Inception V3 models. The dorsal finger knuckle and fingernails of ten concatenated fingers are used to recognize all features extracted by these models. Different similarity metrics are used to compute the matching procedure for every model individually. An evaluation of the proposed approach was performed using datasets consisting of 11,076K hands with left and right hands dorsal, for 190 persons, and 4,650 Poly U, often known as Hong Kong Polytechnic University, Contactless with right hand dorsal for 502 persons. The proposed structure was achieved with results indicating that the Inception V3 models are better than the DenseNet201 model on the 11,076K Hands dataset and the 'Poly U HD' dataset. The left-hand results are better than the right results on the 11,076K Hands dataset and the fingernails produce consistently higher identification results than other hand components, with a rank-1 scores of (99.96% and 96.28%) for inceptionV3 model, (98.11% and 93.42%) for denseNet201 model in the 11,076K Hands dataset and with a rank-1 scores of (97.07%) for inceptionV3 model, (94.83%) for denseNet201 model in the 'Poly U HD' dataset. According to the multi-model deep learning approach proposed in the work, this approach achieved a significant improvement, achieving rank-1 scores of 99.96% compared to previous studies, which plays an important role in knuckle recognition.

Keywords: Pattern Recognition; Personal Identification; Hands Module; Feature Extraction (FE); Deep learning neural network (DLNN)*; *fine-tune (FT); DenseNet201; Inception V3.

1.0 INTRODUCTION

Biometrics is one of the systems for person recognition and is seen as a security system substitute for more conventional techniques like ID cards, passwords, and PIN codes. The technique of identifying a person based on their physiological, behavioral, or chemical traits is made easier by biometrics [1]. Numerous physiological traits have been utilised, including face, fingerprints, iris, and voice. Finger Knuckle Print (FKP) and fingernail (FN) biometric systems are among the many hand-based biometric systems that are gaining popularity because of their high accuracy, computational complexity, dependability, and low cost, especially since they use small imaging devices that require additional hardware [1], [2], [3]. The main benefit of fingernail patterns (FN) is their high degree of distinguishability, even between identical twins as well as between different fingernails on the same person [4]. Because of their great degree of distinctiveness, fingernails can be employed for biometric recognition. However, the anatomical structures of finger knuckle patterns (FKP) are unique. Recently, finger knuckle patterns (FKP) have been researched to improve biometric recognition systems with increased precision [5], [6]. As is often known, using conventional techniques of identity identification, such as ID cards, passwords, and PIN codes, in applications requiring ultimate security is not always the best choice. These traditional techniques, however, have serious drawbacks in that they are susceptible to presentation or spoofing assaults, loss, or theft. Their performance is still inadequate for security applications, despite impressive advancements. One of the most dependable ways to get beyond the preceding problems and allow safe access is to use biometric identification, which has certain

limits. Detection, segmentation, and pattern information extraction are the foundations of person identification in order to locate actual persons. The field of recognition systems studies the combination of biometrics from persons based on their physical and behavioral features and advanced machine learning, such as deep learning neural network (DLNN) [7], [8]. These features can be found in the hand gesture [9], ear [10], face [11], finger vein [12], or a combination of finger vein and knuckle pattern [8].

Deep learning (DL), a branch of "artificial intelligence" (AI), leverages multi-layered neural networks to automatically learn and extract patterns from large datasets. It offers significant advantages, including improved accuracy, the ability to manage complex and large-scale data, and reduced dependency on manual feature extraction (FE). These strengths make DL particularly well-suited for tasks such as image recognition, "natural language processing" (NLP), and predictive analytics. In recent years, DL has gained substantial attention in "computer vision" (CV) [13], [14], especially within the field of biometrics, due to its flexibility and high recognition performance [15], [16], [17]. The primary goal of applying DL in biometrics is to efficiently identify multiple levels of representation by learning discriminative features specific to each biometric modality. A biometric system can apply deep learning at multiple phases, such as interest region extraction (ROI), preprocessing, feature extraction (FE), matching rank, matching, and decision-making. In general, considered, feature extraction (FE) has been the main use of deep learning in biometrics. Multimodal deep learning neural networks (DLNN) have rarely been studied for biometric systems using finger knuckle patterns (FKP) or fingernail (FN). Despite recent advances, multimodal biometrics systems using FKP or FN still have low accuracy and F1_score metrics, difficulty in recognition, and complexity that negatively impact robustness and simplicity. Avoiding all of these problems and improving the recognition performances remains a formidable challenge. Score levels obtained using multiple modalities deep learning for FKP and FN for the same person can perform better than recognition systems that just use FKP or FN. A multimodal biometric system can also process many database templates from enrolled users. To overcome these drawbacks, we need an innovative system for biometric recognition using FKP and FN. FKP and FN biometrics provide secure, contactless, and hard-to-spoof features, making them ideal for high-security systems. Its stability and resistance to surface corrosion also enhance its reliability over time.

In this research paper, a simple and fast approach presents a novel structure for person identification that uses several hand components of the dorsal finger knuckle (Base Knuckle, Major Knuckle, Minor Knuckle) and fingernails. In the proposed structure, the first segmentation of the dorsal finger and fingernails are carried out, which is implemented through a variety of processing steps, including blurring the hand image, converting it to HSV color space, and implementing morphological operations (Dilation Hand Image and Erosion Hand Image), median filtering hand image and using the Hands Module (using the MediaPipe Module). Then, DenseNet201 and Inception V3 models were implemented using the fine-tuned hyperparameters to extract distinctive features. Finally, Hamming Distance (HamD), Jaccard Distance (JaD), Braun-Blanquet Distance (BB), and Bray-Curtis Distance (BC) were used to perform the matching procedure for every model individually.

The following is a summary of the contributions made in the research paper:

1. Introducing a novel structure for person identification based on multi-biometrics of the dorsal finger knuckle and fingernails.
2. Propose a new segmentation method using the Hand Landmark Model (Mediapipe Module).
3. Evaluate the performance of the segmentation method by identifying actual and predicted samples.
4. Investigate several basic CNN models to obtain the best performance based on feature extraction. Then, using the best-performing models, DenseNet201 and Inception V3, fine-tuning was performed on a subset of the 11kHands and PolyUHD datasets based on each hand component (base knuckle, the major knuckle, the minor knuckle, the thumb knuckle, and the fingernails), to enhance feature retrieval.
5. Propose the best matching procedure metrics, Hamming Distance (HamD), Jaccard Distance (JaD), Braun-Blanquet Distance (BB), and Bray-Curtis Distance (BC) to compare the extracted distinctive features.

The remaining sections of the paper will be structured as follows: Section 2 related work, Section 3 materials and methods, Section 4 evaluation results, Section 5 discussion results and Section 6 conclusion and future scope.

2.0 RELATED WORKS

Hand-based biometric systems are commonly used, primarily leveraging features such as fingerprints, palm prints, and finger veins. In contrast, finger knuckle patterns and fingernail biometrics have received less attention, with limited publicly available datasets for these traits. Nevertheless, various feature extractions (FE) and description techniques have been applied to these lesser-studied traits, yielding diverse results in terms of accuracy and performance. Building on this foundation, this research paper also presents a review of previous studies that focus on FE methods used for personal identification, followed by an in-depth study of the most important systems for identifying individuals. Tarawneh et al. [18] introduced a finger knuckle print (FKP) framework that extracts deep features from FKP images using the VGG-19 deep learning model. Merging both deep features (F6 and F7) is also studied using various rules, such as average, maximum, and minimum, using the deep features gathered at layers 6 and 7, both with and without dimensionality reduction tools like the "Principal Component Analysis" (PCA). Experiments conducted on the Delhi Finger Knuckle Dataset achieved an accuracy of up to 95%. The framework

uses a single dataset that can produce results that do not apply to another dataset or real-world scenarios, as diverse datasets can have distinct characteristics and complexities. Chlaoua et al. [19] offered a novel method that uses "principal component analysis network" (PCA Net) to extract features from images of FKP modalities and apply deep learning to construct a multi-modal biometric system. The suggested structure uses PCA to learn a two-stage filter bank, then block histograms and basic binary hashing to cluster feature vectors. These feature vectors are then used as input for classification by a linear multiclass "Support Vector Machine" (SVM). Test results using the FKP dataset from The Hong Kong Polytechnic University (2018) achieved an accuracy of 99.73% and 99.59%. Input images lack quality, as poor lighting conditions, motion blur, or low-resolution images affect the performance of the proposed method, leading to inaccurate feature extraction and classification, which the study may not address.

Zhang et al. [20] used the extraction and assembly of local and global characteristics from FKP images to demonstrate an efficient FKP recognition system. The local feature is specifically marked as the orientation information that was obtained using the Gabor filters. The Fourier transform of the image obtained by extending the scale of the Gabor filter to an infinite value; As a result, the Fourier transform coefficients of an image can be interpreted as its global features. A weighted average of the local and global matching distances determines the final matching distance between two FKP. Experimental results were conducted on the FKP dataset, where the proposed system achieved good results compared to other systems, with a Lower Equal Error Rate (EER) of 0.402% and False Rejection Rate (FRR) of 0.9680%. With improved implementation, this system could become significantly more effective. Usha and Ezhilarasan [21] contribute a novel technique based on geometric and textural studies for personal identification using FKP. In the first method, angular geometric analyses are used to extract the shape-oriented elements of the finger knuckle print, which are subsequently merged to improve the precision rate. In contrast, the multi-resolution transform known as the "Curvelet Transform" (CT) is used to analyse the knuckle texture feature. In this article, each curvelet knuckle is subjected to PCA to recover its feature vector using the covariance matrix resulting from the "Curvelet Coefficients" (CC). Experiments were conducted utilising two datasets (PolyU dataset and IIT finger knuckle dataset), where suggested techniques achieved an accuracy of up to 98.72%. The limitations of this technique are that it requires a higher computational cost than the other techniques, as the texture analysis process takes longer than the geometric analysis technique. Joshi et al. [22] suggested a human authentication system based on the FKP. The research trains a Siamese "Convolutional Neural Network" (CNN) model using pre-processed knuckle ROI images. The suggested system achieved a CRR of 99.24% and an EER of 0.78% on the PolyUFKP database from 165 persons. The Siamese CNN complicates model training and deployment. This complexity may demand more computational resources and experience, limiting its use in low-resource environments.

Sadik, Al-Berry, and Roushdy [23] presented a brief overview of the suggested techniques for FKP-based authentication. Shariatmadar and Faez [24] suggested a system based on FKP images for identity verification and personal identification. Using the "Gabor Filter" (GF), they first extract the features of each finger. Then, they use the PCA algorithm to reduce the dimensionality of the obtained features. After that, they use "Linear discriminant analysis" (LDA) to increase the features' separability. In the finale, they match using the Euclidean distance as a classifier. The identification and verification results of the four-finger feature combination were 98.79% and 91.8% using the Poly U FKP database. The system does not perform well in verification mode, and it takes longer to recognize. Kumar and Xu [25] investigate the dorsal skin patterns on fingers that form between the proximal phalanx and metacarpal bones in order to determine the possibility that they can be used as biometric characteristics. To attain better performance, which may not be achieved using any of these knuckle patterns alone, this study also investigates the simultaneous application of learned or accessible major, first minor, and second minor knuckle patterns. In addition, they examine the potential biometric applications of independent segmented dorsal regions of the palm, obtained in visible illumination. The stability of such second minor finger knuckle patterns is also briefly studied in this paper using a set of images taken more than two years apart. The study achieved EER for matching the dorsal areas of the palm of the hand, which is 0.15607, and this combination index, middle, ring, and little fingers resulted in an EER of 0.096, 0.1054, 0.0994, and 0.1084, respectively, as it was performed on a database of 712 images of the finger dorsal image and 501 different individuals (automatically segmented), for the palm dorsal image. Limited training samples affect matching accuracy from the two sessions, and minor knuckle images are weak and need improvement for forensic purposes. Amina [26] designed a multimodal finger knuckle print identification system using the support vector machine (SVM) classifier and a novel deep learning method known as Discrete Cosine Transform Network (DCT Net). Experiments were conducted using a database of 7920 images from 165 persons, where the system achieved an EER of 3.33% for identification and 7.60% for verification. Environmental issues like illumination conditions and noise may affect the performance of the Finger-Knuckle-Print identification system. In contrast, these issues are not addressed in the research. Conditional variations may lead to variable recognition rates.

Zhang, Zhang, and Zhang [27] introduce a new FKP-based system for personal identity authentication. To obtain the FKP images, a specialized data acquisition device is designed, and then the FKP recognition algorithm is used to process the data obtained. The FKP image's local convex direction map is extracted, from which a coordinate system is determined to align the images and, a region of interest (ROI) is cropped for feature extraction. The FKP features are extracted and represented using a competitive coding scheme that employs a 2D GF to extract

the image local orientation information. When matching, the angular distance is applied to evaluate the degree of similarity between two images' competitive code maps. Experiments were conducted on 5,760 images of 480 different fingers, where the FKP recognition system achieved a true acceptance rate (97%) and a low false acceptance rate (0.02%). The system lacks high-quality image samples, which affects the matching accuracy.

A. Attia, et al. [28] propose a novel approach described as "Log Gabor-TPLBP" (LGTPLBP). Nonetheless, the FKP identification system was implemented using the "Three Patch Local Binary Patterns" (TPLBP) approach utilised for face recognition, which can be applied to FKP recognition. The real and imaginary images have been extracted from each "Region of Interest" (ROI) of the FKP images using the 1D-Log Gabor Filter. The feature vectors of the real image and the hypothetical image, respectively, were then extracted using the TPLBP descriptor on both images. For every FKP image, these feature vectors have been joined to create a sizable feature vector. Subsequently, all of the acquired feature vectors are immediately processed via a linear discriminant analysis (LDA) dimensionality reduction procedure. Lastly, during the matching stage, the cosine Mahalanobis distance (MAH) has been employed. The system achieved an accuracy of 99.60% and 99.80% using the Hong Kong Polytechnic University (PolyU) FKP database. Although the system utilises Linear Discriminant Analysis (LDA) for dimensionality reduction, this approach may face challenges with high-dimensional data, particularly when the sample size is small relative to the number of features. This can result in overfitting or the loss of key discriminative information. Chalabi, Attia, and Bouziane [29] propose a finger dorsal knuckle print multimodal identification system. To gain a better understanding of the exploited characteristic, they extract features from both the minor and major finger dorsal knuckles using PCA Net. Subsequently, SVM is employed for the two modalities' matching stage, and a score-level fusion method is used to merge the scores using distinct rules. Experiments were performed on the publicly available PolyUKV1 database, which achieved a rank-1 accuracy of 93.44%. Using PCA Net with an SVM classifier may lead to computational complexity, which may limit the scalability and practical performance of the system. Most existing research using deep learning, which relies on segmentation methods, requires a large amount of labeled data for the training network, which is often challenging for large datasets. It is important to emphasize that research conducted on fingernails through hand images has not received much attention in the field of biometric systems. The ability of nails to change may be one factor. Despite there are many FKP recognition methods in the literature, none of them is perfect and each has its own set of drawbacks, which are often inherited from problems carried over from computer vision (CV) and machine learning (ML). As a result, there is still space for development, particularly when applying deep learning methods to FKP and FN images.

3.0 MATERIALS AND METHODS

This section focuses on the methodology for creating and using the finger knuckles and fingernails recognition multimodal. This research paper presents deep learning neural network (DLNN) methods for biometric recognition of finger knuckle patterns and fingernails.

3.1 Brief Description of the Dataset

In this research paper, the performance of a convolutional neural network is evaluated using the ’11-k Hands’ dataset and the Hong Kong Polytechnic University contactless hand dorsal Images dataset.’11k Hands’ dataset [25], which includes 11076 hand images from 190 persons, which comprises in the dorsal and palmar views. The hands in the images are in a variety of hand positions, from widely opened to partially closed to closed. Using a USB document camera with a resolution of 1600 × 1200 pixels, each image in this database was taken with the hands at about the same distance from the camera. Furthermore, as the subject of this work is finger knuckles and fingernails, the 2738 left and 2755 right dorsal images have been chosen. PolyUHD dataset [30] includes 4650 hand dorsal images of 501 persons’ right hands in a comparable flat position with open fingers, making up this database. With a hand-held camera, the 1600 x 1200 pixel images were taken under both indoor and outdoor lighting conditions.

In this work, we tested different CNN models to develop more accurate models that can be used for the recognition of finger knuckle patterns and fingernail images. Only the dorsal parts for person identification in the 11k Hands and PolyU HD datasets are of interest to us in this work. The dorsal numbers for the right and left hands are 2738 and 2755, respectively. For training, validating and testing the fine-tuned model, we used 52,022 and 52,345 segmented images from the left and right dorsal in the 11k Hands database, respectively. The dorsal hand number is 4650 on the right. We used 88,350 segmented images from the right dorsal in the PolyUHD dataset for the training, validation and testing of the fine-tuned model, respectively. To avoid over-fitting and to guide the training process, the classes are divided into two parts. The first part of the data comprises (70%) of the data to train the model, the remaining part (30%) of the data is utilised to validate the training model, and the data that will be utilised to test the model constitutes (30%).

3.2 Modeling Architectures

Recently, advances in deep learning neural networks (DLNN), especially in the field of biometrics, propose that several Deep CNN architectures may be used [31]. However, convolutional neural networks (CNNs) can be challenging to train from scratch. To overcome this problem, this work uses a diversity of pretrained models and transfer learning techniques. The main benefit of transfer learning is its ability to train data more quickly and with fewer samples. The information acquired by the previously trained model can be applied by the newly trained model [32]. This work includes a comprehensive evaluation of two different baseline models. Some examples of these baseline models are DenseNet201 and Inception V3. Due to their effective use in computer vision, these models were chosen. Adding the fine-tune to make each baseline model appropriate for the number of classes used in the experiments allowed for their usage as transfer learning models in this work. In the following subsections, each of these various models will be briefly discussed.

3.2.1 DenseNet201 Architecture

Dense connections are a characteristic of the Dense Net architecture. By linking every layer to every other layer, it enhances Res Net architecture [33]. In these densely linked architectures, each layer receives feature maps from each layer that comes before it and transmits its own feature map to the one above it. Reusing features with an overall minimum amount of parameters is another important benefit of this kind of architecture. The DenseNet201 architecture, which was used in this work, is one of the many commonly used versions of the Dense Net architecture. (see original DenseNet201 Model in Fig. 1).

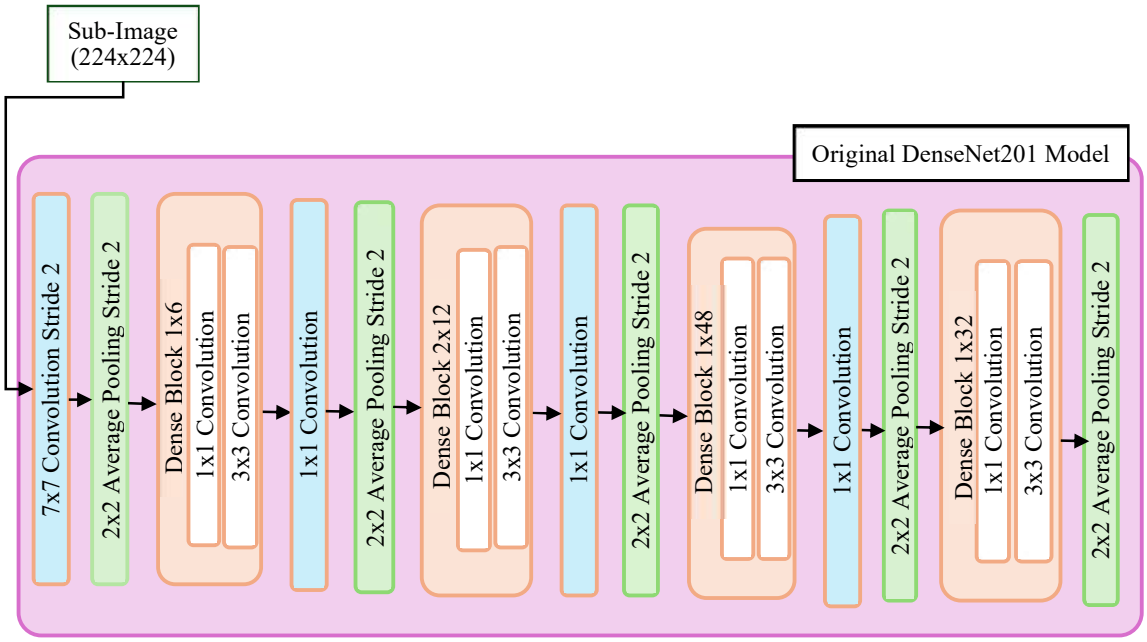

Fig. 1: DenseNet201 architecture

3.2.2 InceptionV3 Architecture

The fundamental idea underlying the InceptionV3 architecture is to "widen" the network by allowing it to contain many different types of kernels on the same level, which addresses the problem of excessive variability in the position of the prominent sections in the images under evaluation. This idea of several kernels functioning at the same level is made possible by the so-called Inception modules. Using this basic idea, the first InceptionV1 (Google Net) was proposed [34]. The InceptionV1 architecture was later expanded upon by the InceptionV2 and InceptionV3 architectures, which were introduced in [35]. These improvements included adding kernel factorization, batch normalization to auxiliary classifiers, and resolving representational bottlenecks and auxiliary classifiers. First runner-up in the ILSVRC 2015 image classification test went to this InceptionV3 architecture. (see original InceptionV3 Model in Fig. 2).

3.3 Proposed Approach

In our approach, this work used a multimodal deep learning neural network (DLNN)-based structure to recognize dorsal finger knuckle and fingernails using the DenseNet201 model and Inception V3 model, supported by fine-tuning of feature extraction (FE). To the best of our knowledge at the time of publication, no literature had taken this idea into consideration. Based on the achievement of deep learning neural network (DLNN) in solving many complex tasks, this enhanced structure aims to achieve optimal recognition of finger knuckle and fingernails by highlighting missing details in knuckle images against the restrictions such as noise, blur, and brightness. A schematic diagram of the proposed structure is shown in Fig. 3. The first to third phases of the structure are: 1. Pre-processing; 2. Feature extraction (FE); and 3. Evaluation of matching and similarity.

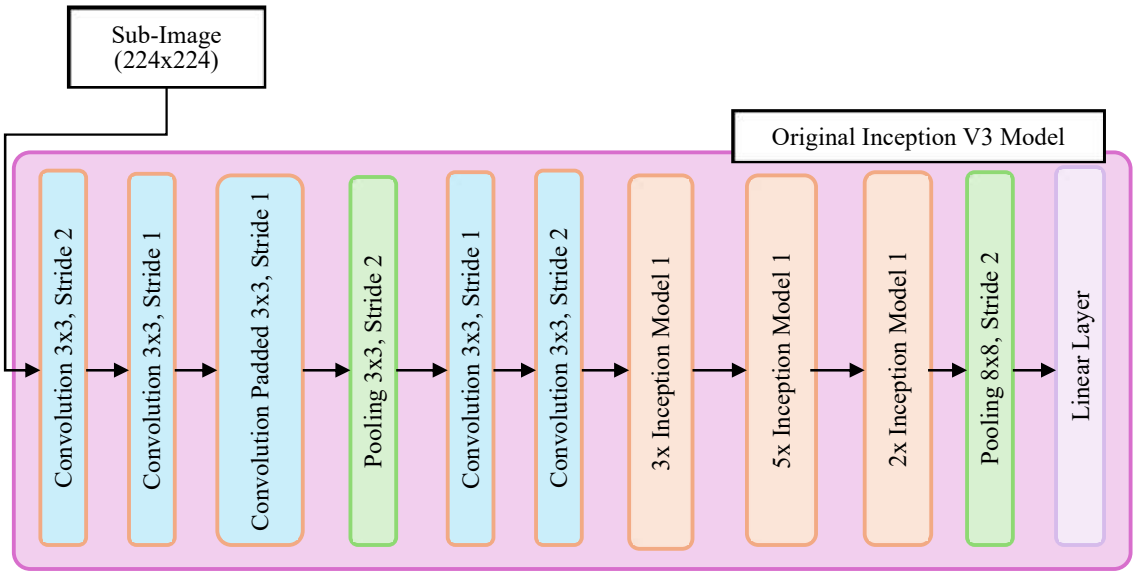

Fig. 2: InceptionV3 architecture

3.3.1 Pre-Processing Phases

This phase detects the dorsal finger knuckle patterns and fingernails from the image of the hand. In this work, using the hands module (MediaPipe Module) for hand posture estimation is the approach dedicated to this purpose in order to detect the location of a hand area, such as finger knuckle patterns and fingernails. The main components of the hand are detected through the key points of this model. To achieve the best result of localization key points, the original manual image was resized to 224x224. The process of detecting the dorsal finger knuckle patterns and fingernails is illustrated in Fig. 4.

According to Fig. 4, the process of detecting the dorsal finger knuckle and fingernail patterns is implemented through a variety of processing steps as in:

(i) Apply blurring hand image: An image can be made blurrier by applying a Gaussian Blur filter to it, which reduces the amount of noise in the image. One crucial component of image processing is image blurring [36], [37].

(ii) Convert to HSV color space: The objective of this sub-step is to identify the skin region in the hand image by first converting the RGB to HSV color space and then applying certain skin area determination rules [38], [39], [40].

(iii) Apply morphological operations: It consists of a set of processes that use shapes to process images. Once an input image has been given a structural element, it produces an output image. Two of the most fundamental morphological processes are dilation and erosion [41], [42], [43].

(iv) Apply median Filtering: It is excellent at lowering this kind of noise. The filtering technique uses a small matrix (such as a 3x3) to scan the entire image. It then uses the median of all the values inside the matrix to recalculate the value of the center pixel [44], [45], [46].

(v) Finally, detect the dorsal finger knuckle and fingernail patterns. Use hands Module (MediaPipe Module): It is a high-precision method for tracking fingers and hands. It uses machine learning (ML) to deduce nine 2D hand landmarks from a single frame [47], [48].

After completing the four processing steps, cropped sub-images of the hand's keypoints will be generated as shown in Fig. 5. Every hand consists of 19 various components, namely:

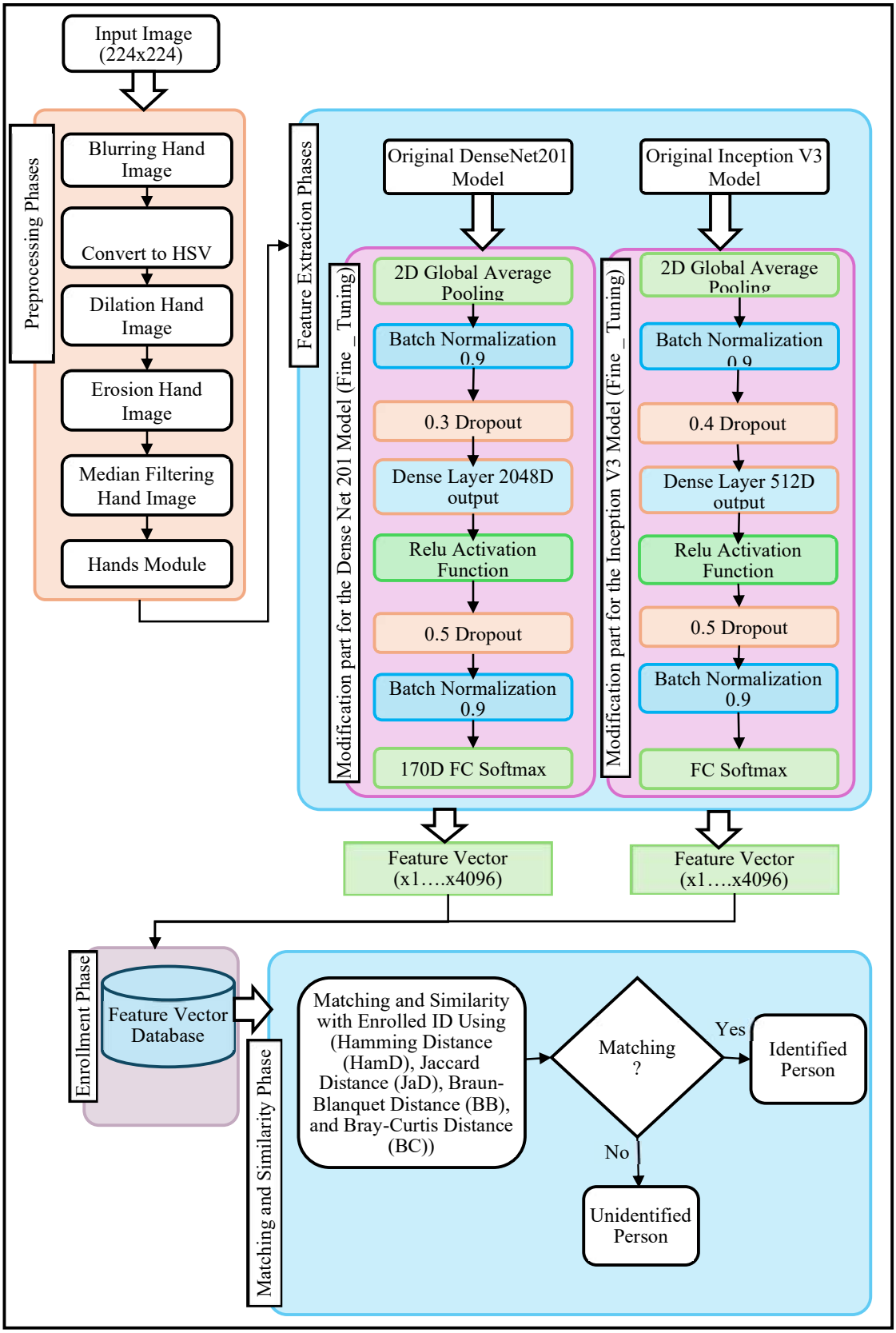

Fig. 3: A schematic diagram of the structure for personal identification based on (FKP & FN)$^{+}$

(a) Five base knuckle, or metacarpophalangeal (MCP) joints.
(b) Four major knuckle or proximal interphalangeal (PIP) joints.
(c) Four minor knuckle or distal interphalangeal (DIP) joints.
(d) One minor knuckle of the thumb or interphalangeal (IP) joints.
(e) Five fingernails.

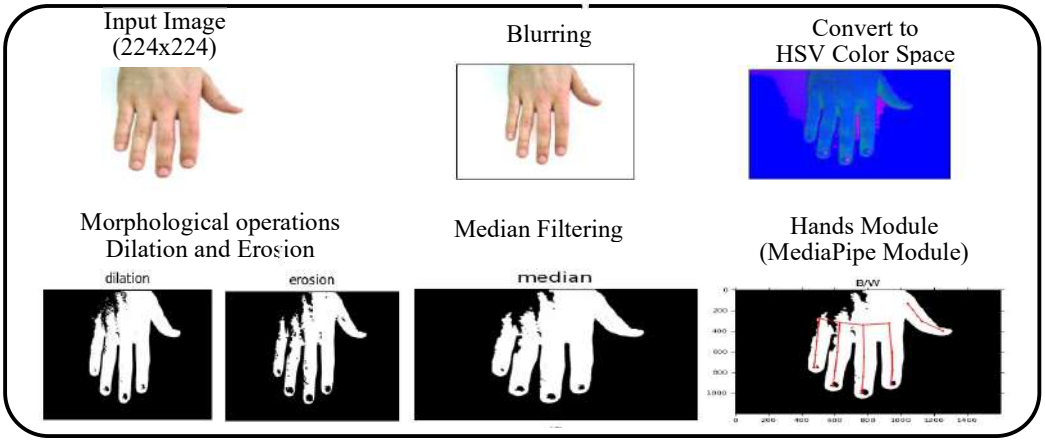

Fig. 4: Shows the processing steps for detecting the dorsal finger knuckles patterns and fingernails

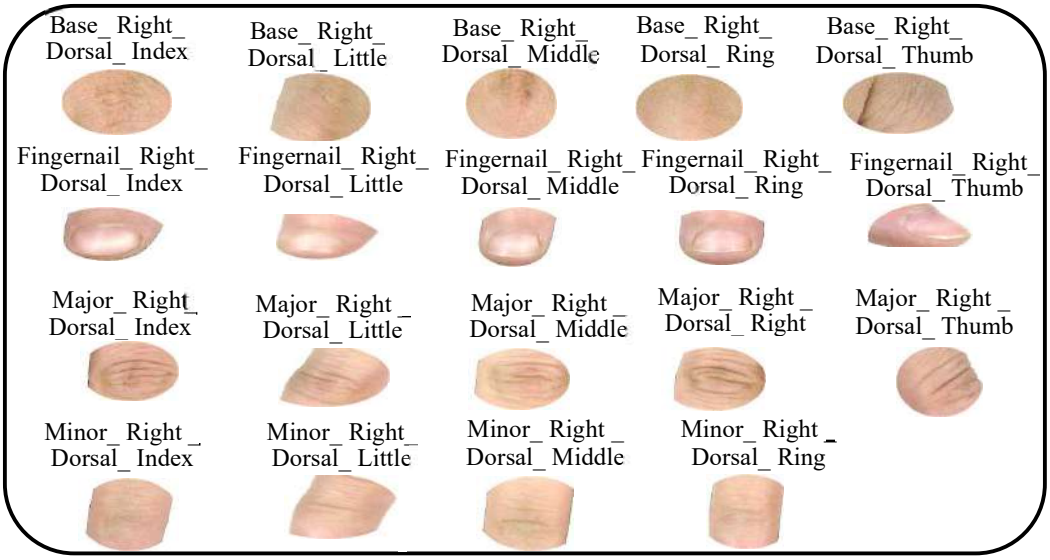

Fig.5: Shows the sample of the sub-images of the hand's keypoints

3.3.2 Feature Extraction (FE) Phases

Any pattern recognition system must include feature extraction because it is essential to achieving high-performing findings. Obtaining features of unevenness and distinctiveness is crucial in order to distinguish between various patterns [21], [49]. Thus, in this work, the proposed approach uses fine-tuning of the Dense Net201 model and fine-tuning of the Inception V3 model (see Fine _ Tuning in Fig.3) to extract the feature vectors for each model separately and performs them on each keypoints hand components separately and as well as merging all dorsal Finger Knuckles Patterns and Fingernails (FKP & FN)$^{+}$ for left hand and right. The configurations of the hyperparameters and parameters chosen for the DenseNet201 model and Inception V3 model are presented in Table 1. The pre-trained models DenseNet201 and Inception V3 were first loaded. A convolution was then performed using a 224 x 224 input image, freezing the ImageNet weights for feature extraction and transfer learning. From the initial DenseNet201 model, the first 700 layers were frozen. In this work, freeze some of the 48 layers in Inception V3. Then, the Global average pooling(GAP) layer, flatten layer, and fully connected (Dense)

layers were fine-tuned. In this work, an output layer with a softmax activation function is utilised for finger knuckle patterns and fingernails (FKP & FN)+ recognition. In addition, training is enhanced by adding a batch normalization layer and a dropout layer to prevent overfitting.

Table 1: DenseNet201 and Inception V3 hyper parameters value

	DenseNet201	**Inception V3**
Hyper parameters	**Value**	
Input Size	224 x 224	224 x 224
Batch Size	16	16
Seed	1337	42
Optimizer	Adam	Adam
Learning-Rate	1e-2	1e-3
Epochs	100	100
Loss Function	Binary- Cross Entropy	Binary- Cross Entropy
Dense	2048	512
Total Parameters	26,988,797 (Use 11K Databases) 28,262,964 (Use PolyUHD Database)	22,948,829 (Use 11K Databases) 23,108,372 (Use PolyUHD database)
Trainable Parameters	8,654,781 (Use 11K Database) 9,928,948 (Use PolyUHD Database)	13,958,717 (Use 11K Database) 14,118,260 (Use PolyUHD Database)
Non-Trainable Parameters	18,334,016 (Use 11K Database & PolyUHD Database)	8,990,112 (Use 11K Database & PolyUHD Database)

3.3.3 Evaluation of Matching and Similarity Phase

To attempt to solve pattern recognition problems, metrics of similarity and distance (dissimilarity) are essential [50]. Various mathematical techniques are used to measure the proximity or distance between two objects at their respective locations in order to make similarity and distance measurements [56]. In the third phase, several metrics such as Hamming Distance (HamD), Jaccard Distance (JaD), Braun-Blanquet Distance (BB), and Bray-Curtis Distance (BC) are used with the basic model feature extractor described previously. Performance is then further enhanced using the best recognition results for the subsequent fine-tuning phase. The opposite of the distance metric between two vectors is the similarity metric, which states that the degree of similarity increases with decreasing distance and vice versa. In this paper, feature extractors are used, where these hand parts are first mapped onto feature spaces. The length of each feature vector is 4096. Second, persons were matched per hand component using the similarity metrics. The proposed system's recognition performance is evaluated using the Hamming distance (HamD) [51], [52], Jaccard distance (JaD) [52], [53], Braun-Blanquet Distance (BB) [50], [53], and Bray-Curtis (BC) [54], [55] metrics. It is described by the following equations (1-4).

Hamming Distance (HamD): $HamD(x, y) = \sum_{i=1}^{n} 1_{xi \neq y}$ (1)

Where

x&y: The two strings or binary sequences, n: the length of the strings (or sequences),

x_i& y_i: the elements (bits) at the i-th position in the strings x and y

Jaccard Distance (JaD): $J(A, B) = \frac{|A \cap B|}{A \cup B}$ (2)

Where

A and B are two sets,

$|A \cap B|$ is the number of common elements in both sets.

$|A \cup B|$ is the total number of unique elements in both sets.

Braun–Blanquet Distance (BB): $S(A, B) = \frac{|A \cap B|}{\max(|A|, |B|)}$ (3)

Where

$|A \cap B|$is the number of common elements in both sets.

$|A|$ $|B|$ are the sizes (cardinalities) of sets A and B.

max $(|A|, |B|)$ is the size of the larger set.

Bray-Curtis Distance (BC): $S_{BC} = \frac{(b+c)}{2a+b+c}$ (4)

Where a, b, and c represent the abundance of features

The dorsal FKP & FN algorithm explains the method used to identify a person and summarizes the suggested structure (FKP & FN)$^{+}$ step by step.

Algorithm (Dorsal FKP & FN) : suggested (FKP & FN)$^{+}$ framework
Input: Dataset 11k Hands, PolyUHD
Output: Personal Identification

Begin
Step1: Read the hand image from the 11k Hands and PolyUHD Dataset
Step2: FOR each row (I) from 1 to 224 pixels (image height)
Step3: FOR each column (J) from 1 to 224 pixels (image width)
Step4: **Pre-Processing Phases**
Step4-1: While the hand image (I) is available, do
Step4-2: Segmenting the finger knuckle patterns and fingernails
Step4-3: Apply the blurring hand image
Step4-4: Convert to HSV color space
Step4-5: Apply morphological operations (dilation and erosion)
Step4-6: Apply median filtering
Step4-7: Use the hand landmark model (Mediapipe Module)
Step4-8: **END FOR (J)**
Step4-9: **END FOR (I)**
Step4-10: Return Final Result
Step5: Create a database with sub-images of every component.
Step6: **Feature Extraction (FE) Phases**
Step6-1: for $p \leftarrow 1$ to 19 do
Step6-2: Divide the database into three distinct sets: testing, validation, and training classes for model evaluation and training.
Step6-3: Set the network configuration (DLNN apply modification part for denseNet201 Model, modification part for inceptionV3 Model)
Step6-4: Create augmentation images on the validation and training sets
Step6-5: Using specific epochs to train.
Step6-6: Determine the network weight (W) that achieves the highest validation accuracy and F1_ Score
Step6-7: Using the weight (W), extract the features from the pairings (a) and (b) for further analysis.
Step7: **Evaluation of Matching and Similarity Phase**
Step7-1: Compute the similarity metrics using the matching equations:
Step7-2: if
Calculate the number of bit differences between features using the Hamming Distance (HamD) in Equation (1).
Step7-3: then
Calculate the measures of the similarity between two sets using Jaccard Distance (JaD) in Equation (2).
Step7-4: **END**
Step7-5: if
Calculate the measures of the similarity between two sets using Braun–Blanquet Distance (BB) in Equation (3).
Step7-6: then
Calculate the sum of absolute differences between features relative to their total sum using Bray-Curtis Distance (BC) in Equation (4).
Step7-7: **END**
Step8: **Return the calculated distance values for HamD, JaD, BB, and BC.**
Step9: **END**

4.0 EVALUATION AND RESULTS

The main goal of this evaluation is to determine how efficient and accurate our approach is in identifying a person. Evaluate our approach in three steps in this section. The evaluations were performed on a computer equipped with an 11th Gen Intel Core i7-1362OH processor, 16 GB of RAM, a 512 GB SSD NVME, and Windows 11, which is adequate for executing Python 3.9 and managing data-intensive activities. Python library frameworks, such as

PyTorch and TensorFlow, leverage the performance of Nvidia GPUs' for deep learning and machine learning applications.

- Evaluation of the segmentation method
- Evaluation of multi-model deep learning neural network (DLNN)
  - Model Evaluation
  - Evaluation of the DenseNet201 model
  - Evaluation of the Inception V3 model
- Evaluation of Similarity and matching

4.1 Evaluate the Segmentation Method

The results of the segmentation methods for finger knuckle patterns and fingernails proposed in the pre-processing phase are evaluated in this subsection. Table 2 shows the accuracy for the dorsal the right and left hands using the hands' landmark model.

Table 2: A demonstration of the accuracy for the 11KHands dataset & PolyUHD dataset

	Actual	Predicted	Accuracy
Dorsal Left Hand_11k Hand dataset	2738	2688	**98.174%**
Dorsal Right Hand_11k Hand dataset	2755	2618	95.027%
Dorsal Right Hand_ PolyUHD dataset	4650	4538	**97.112%**

We observe from our experiments that the results were higher and excellent in the left-hand dorsal in the 11k dataset compared to the right-hand dorsal in the 11k hand and the PolyUHD datasets. The actual and predicted values for all samples in the two datasets in Fig. 6 explained the best accuracy. These results are further justified by the integration of robust deep learning models, such as DenseNet201 and Inception V3 models, which enable deep feature extraction, and the use of multiple similarity measures (Hamming Distance (HamD), Jaccard Distance (JaD), Braun-Blanquet Distance (BB), and Bray-Curtis Distance (BC)), which enhance recognition accuracy by offering diverse perspective in feature comparison.

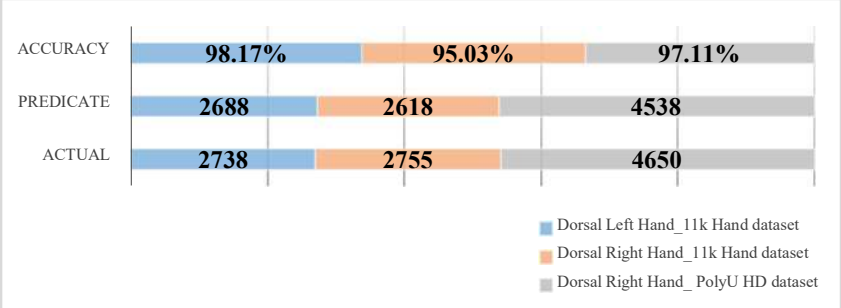

Fig. 6: Shows result accuracy for 11K Hands and PolyUHD datasets

4.2 Evaluation of Multi-Model Deep Learning Neural Network (DLNN)

We experiment with several base models, such as CNNN (Convolution Neural Network), pretrained to extract the features from finger knuckles and fingernails. In the subsection, the results of the multimodal deep learning neural network (DLNN) will be evaluated: The DenseNet201 model and the Inception V3 model will be evaluated after fine-tuning of each model is added to the extracted features.

4.2.1 Model Evaluation

• Confusion Matrix (CM): The efficiency of the network architecture of each model was evaluated by using confusion metrics. The confusion matrix is a table that summarizes the prediction results of a classification problem, as shown in Fig. 7. There are four categories based on the number of accurate and inaccurate predictions [56], [57], [58], [59], [60], [61].

True positive (TP): The predicted and actual results are both positive.
False positive (FP): When there is a positive prediction but a negative actual result

True negative (TN): The predictions and the actual result are both negative.
False negative (FN): Although a negative result was predicted, a positive result was achieved.

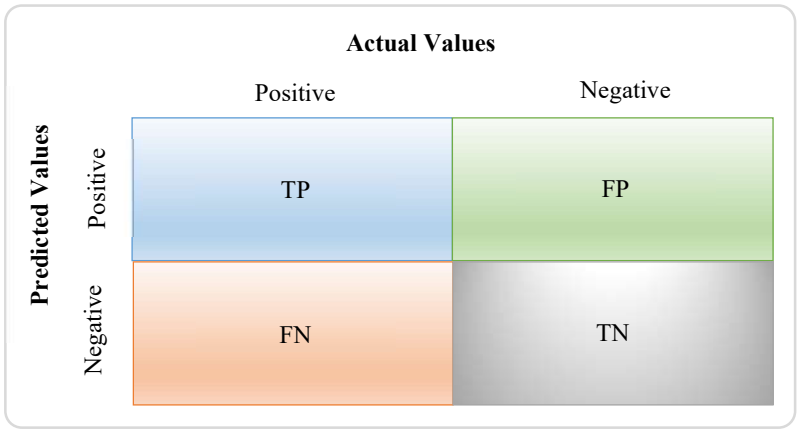

Fig.7: An illustration of the confusion matrix

• Classification Metrics (CM): The five metrics mentioned below were used to evaluate the performance of the models [62], [63], [64], [65].

Accuracy (AUC): is the percentage of accurate to inaccurate predictions.

$$\text{Accuracy(AUC)} = \frac{T_P + T_n}{T_P + T_n + F_p + F_n} \quad (5)$$

Precision (PPV): demonstrates the accuracy with which a model classifies a sample as positive.

$$\text{Precision(PPV)} = \frac{T_P}{T_P + F_p} \quad (6)$$

Recall (Sensitivity): the ability of a model to identify positive samples

$$\text{Recall (Sensitivity)} = \frac{T_P}{T_P + F_n} \quad (7)$$

Specificity(SPC):

$$\text{Specificity(SPC)} = \frac{T_n}{T_n + F_p} \quad (8)$$

F1 score: evaluates the balance between the precision and recall values.

$$\text{F1\_Score} = \frac{2 * T_P}{2 * T_P + F_p + F_n} \quad (9)$$

Micro-Averaged: Every sample contributes the same amount to the final averaged metric.
Macro-Averaged: Every class contributes an equal amount to the averaged final metric.
Weighted-Averaged: The weighting for every class's contribution to the average depends on its size.

4.2.1.1 Evaluation of the DenseNet201 Model

The main datasets are divided into subsets for testing, validation, and training. After each training cycle, the proposed models are verified against the validation set and trained using training data. After that, we evaluate the models using the testing dataset and use evaluation metrics to measure the DenseNet201 model's performance. Fig. 8 offers accuracy and F1-score for each dorsal finger knuckle pattern and fingernail use, multi-classification for the DenseNet201 Model.
After obtaining superior multi-classification for each key component in both the 11k left and right dorsal hands dataset and the Poly UHD right dorsal hands in the DenseNet201 model, we obtained the summarized classification results for each key component in both the 11k left and right dorsal hands dataset and the PolyUHD right dorsal hands in the DenseNet201 model. Tables 3, and 4 illustrate a summarized classification for the DenseNet201 model (11k Hands for (Left Dorsal & Right Dorsal) and PolyUHD for (Right Dorsal)). Fig. 9 offers a summarized classification for training and testing for the DenseNet201 model (11k Hands for (11k Hands for (Right Dorsal & Left Dorsal) and PolyUHD for (Right Dorsal)).

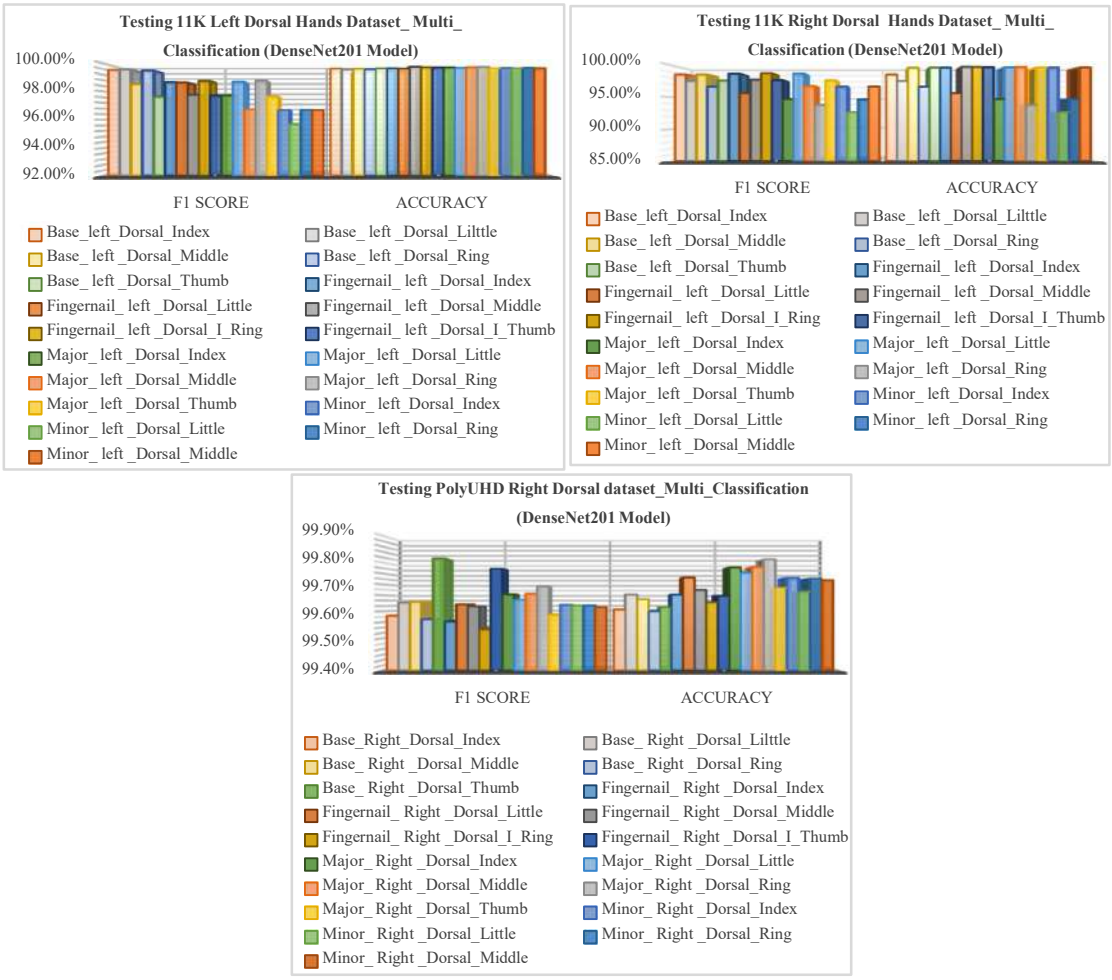

Fig.8: Shows accuracy and F1-score for each dorsal finger knuckle pattern and fingernail based on the DenseNet201 model

Table 3: Show accuracy and F1-score (summarized-classification-report training & report testing) for DenseNet201 model (11kHands (left dorsal &right dorsal))

	Summarized-Classification for DenseNet201 Model-11k Hands (Left Dorsal)					
	Report Training			**Report Testing**		
	Micro%	Macro%	Weighted%	Micro%	Macro%	Weighted%
Precision	85.87%	88.12%	88.10%	87.85%	90.10%	90.11%
Recall	85.87%	85.93%	85.87%	87.85%	87.86%	87.85%
F1_Score	85.87%	85.84%	85.79%	87.85%	87.84%	87.83%
Accuracy	85.87%	85.87%	85.87%	87.85%	87.85%	87.85%
	Summarized-Classification for DenseNet201 Model-11k Hands (Right Dorsal)					
	Report Training			**Report Testing**		
	Micro%	Macro%	Weighted%	Micro%	Macro%	Weighted%
Precision	94.25%	94.98%	94.98%	92.97%	94.42%	94.42%
Recall	94.25%	94.25%	94.25%	92.97%	92.97%	92.97%
F1_Score	94.25%	93.77%	93.77%	92.97%	92.94%	92.94%
Accuracy	94.25%	94.25%	94.25%	92.97%	92.97%	92.97%

Table 4: Show accuracy and F1-score (summarized-classification-report training & report testing) for DenseNet201 Model (PolyUHD (Right Dorsal))

	Summarized-Classification for DenseNet201 Model-PolyUHD (Right Dorsal)					
	Report Training			**Report Testing**		
	Micro%	Macro%	Weighted%	Micro%	Macro%	Weighted%
Precision	94.09%	94.52%	94.57%	93.48%	94.22%	94.25%
Recall	94.09%	94.05%	94.09%	93.48%	93.49%	93.48%
F1_Score	94.09%	93.88%	93.93%	93.48%	93.50%	93.51%
Accuracy	94.09%	94.09%	94.09%	93.48%	93.48%	93.48%

Fig. 9: Show a summarized classification for training & testing for the DenseNet201 model

4.2.1.2 Evaluation of the Inception V3 Model

We evaluate the models using the testing dataset and use evaluation metrics to measure the Inception V3 model's performance. Fig. 10 offers accuracy and F1_Score for each dorsal finger knuckle pattern and fingernail use multi-classification for the Inception V3 model.

After obtaining superior multi-classification for each key component in both the 11k left and right dorsal hands dataset and the PolyUHD right dorsal hands in the Inception V3 model, we obtained the results for summarized classification for each key component in both the 11k left and right dorsal hands dataset and the PolyUHD right dorsal hands in the Inception V3 model. Tables 5, and 6 illustrate a summarized classification for the denseNet201 model (11k Hands for (Left Dorsal & Right Dorsal) and PolyUHD for (Right Dorsal)). Fig. 11 offers a summarized classification for training and testing for the Inception V3 Model (11k Hands for ((11k Hands for (Right Dorsal & Left Dorsal) and PolyUHD for (Right Dorsal)).

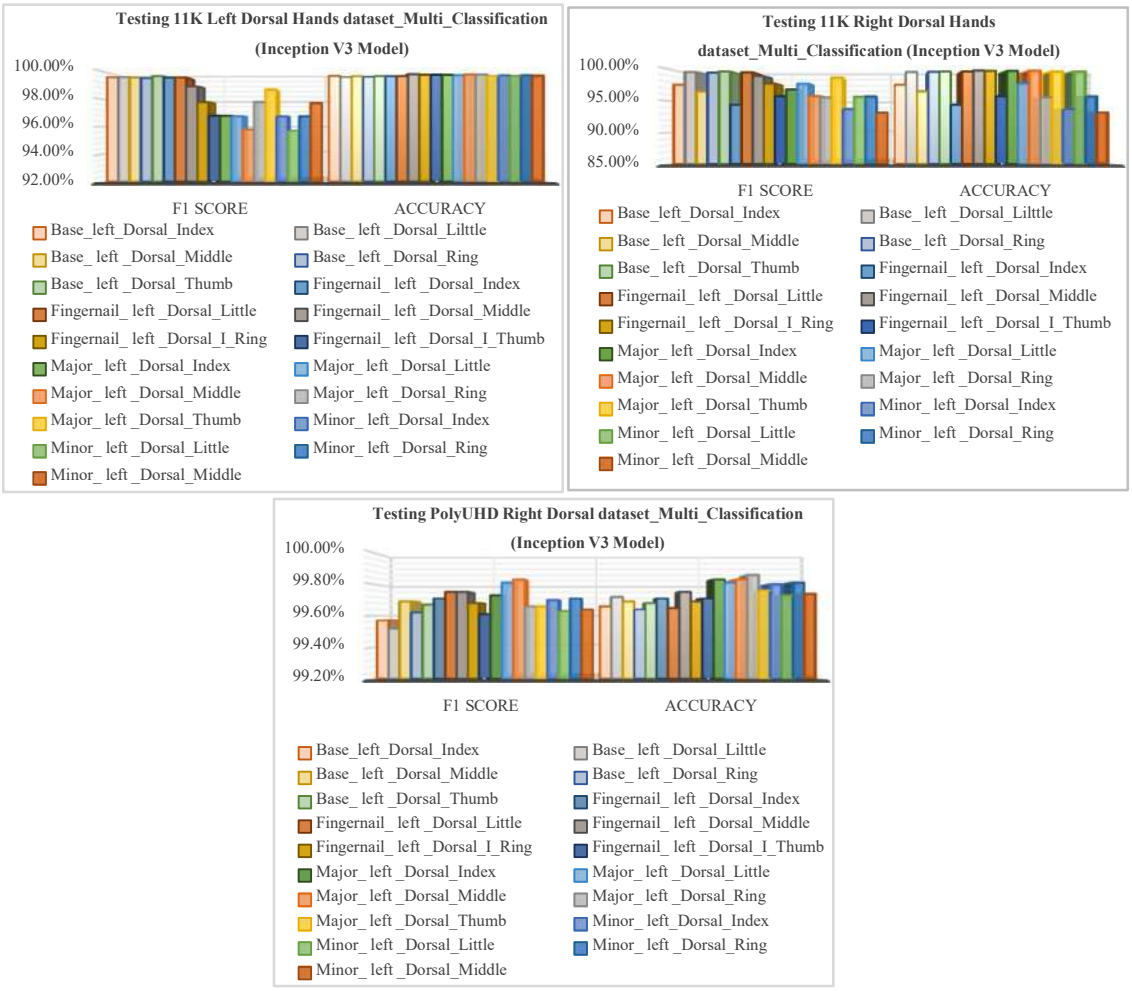

Fig. 10: Shows accuracy and F1-score for each dorsal finger knuckle pattern and fingernail based on Inception V3 models

Table 5: Show accuracy and F1-score (summarized-classification-report training & report testing) for Inception V3 model (11k Hands (left dorsal &right dorsal))

	Summarized_ Classification for Inception V3 Model_ 11k Hands (Left Dorsal)					
	Training			**Report Testing**		
	Micro%	Macro%	Weighted%	Micro%	Macro%	Weighted%
Precision	95.25%	95.56%	95.56%	95.44%	95.81%	95.81%
Recall	95.25%	95.25%	95.25%	95.44%	95.44%	95.44%
F1_Score	95.25%	95.25%	95.25%	95.44%	95.39%	95.39%
Accuracy	95.25%	95.25%	95.25%	95.44%	95.44%	95.44%
	Summarized_ Classification for Inception V3 Model_ 11k Hands (Right dorsal)					
	Report Training			**Report Testing**		
	Micro%	Macro%	Weighted%	Micro%	Macro%	Weighted%
Precision	91.87%	94.08%	94.08%	91.67%	93.51%	93.51%
Recall	91.87%	91.87%	91.87%	91.67%	91.67%	91.67%
F1_Score	91.87%	92.17%	92.17%	91.67%	91.84%	91.84%
Accuracy	91.87%	91.87%	91.87%	91.67%	91.67%	91.67%

Table 6: Show accuracy and F1-Score (summarized-classification-report training & report testing) for DenseNet201 model (PolyUHD (right dorsal))

	Summarized-Classification for Inception V3 Model-PolyUHD (Right Dorsal)					
	Report Training			**Report Testing**		
	Micro%	Macro%	Weighted%	Micro%	Macro%	Weighted%
Precision	98.47%	98.58%	98.58%	95.44%	96.64%	96.64%
Recall	98.47%	98.47%	98.47%	95.44%	95.44%	95.44%
F1_Score	98.47%	98.47%	98.47%	95.44%	95.59%	95.59%
Accuracy	98.47%	98.47%	98.47%	95.44%	95.44%	95.44%

Fig.11: Show a summarized-classification for training & testing for the Inception V3 model

The DenseNet201 and Inception V3 models were trained to classify right dorsal and left dorsal hands, are 2755 and 2738 images for the 11K hands dataset after models were trained to classify 502 classes for 4650 images for the PolyUHD right dorsal dataset. Initially, images of size 224 × 224 pixels were used as the input to the models and trained for 100 epochs. The accuracies, F1-score, and loss obtained on the training, validation sets are presented for some samples in Fig. 12. The efficiency of each model's evaluation using the Confusion matrix is shown in Fig. 13.

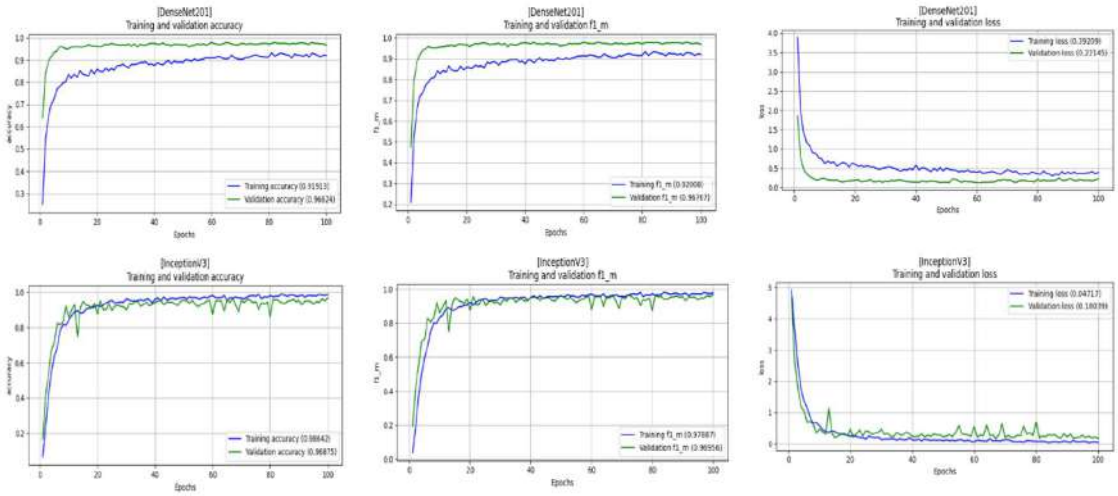

(a) (b) (c)

Fig. 12: Show result for DeneNet201 model & Inception V3 model (Fingernail-Right-Dorsal-Index-11KHand (right dorsal) & PolyUHD (right dorsal)): (a) training accuracy& validation accuracy, (b) training F1-Score & validation F1_Score, (c) training loss & validation loss

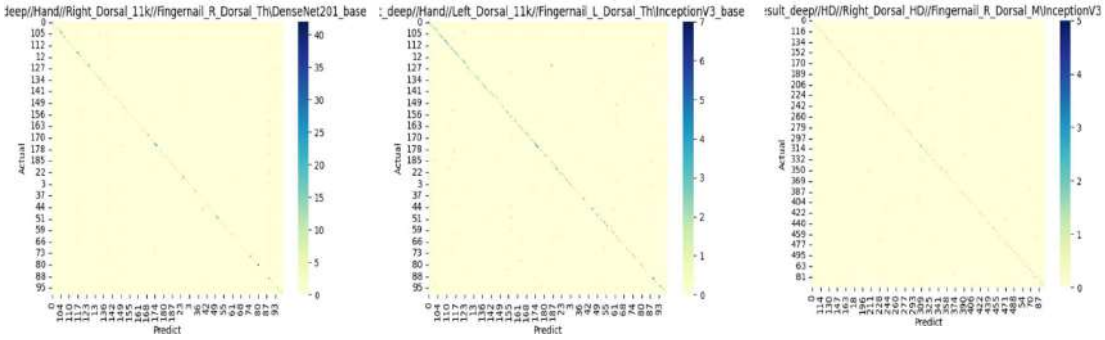

Fig.13: Confusion matrix for some samples 11KHands and PolyUHD for dorsal finger knuckle pattern and fingernails using DenseNet201 & Inception V3 models

4.3 Evaluation of Similarity and Matching

A phase in the matching process is estimating the similarity between two sub-images of the identical hand. One segmented image from the query may match with one or more corresponding segmented images in the library throughout the matching process. Using the feature vectors obtained from the previous phase, we evaluated the similarity using a rank-1 recognition rate. The definition of the rank-1 of recognition is as follows:

$$rank - 1 = \frac{N_i}{N} x100 \tag{10}$$

The total number of samples that were attempted to be recognized is N, and the number of samples that were accurately allocated to the appropriate person is Ni. Using various pretrained models and similarity distances, Table 7 shows the rank-1 recognition accuracy of an 11k hands database (shown as a percentage). Table 8 illustrates the rank-1 recognition rate (shown in %) for the 11k Hands and PolyUHD dataset.

Table 7: Show a comparison between different pre-trained models and similarity distances for the rank-1 recognition accuracy of 11k Hands and PolyUHD datasets

Bray-Curtis Distance					
Finger	**Model**	**Rank-1**	**Finger**	**Model**	**Rank-1**
	Base_ Left_ Dorsal			**Major_ Right_ Dorsal**	
Thumb	DenseNet201	87.83	Index	MobileNetV2	86.70
Index	ResNet50V2	82.01	Little	DenseNet169	100
	Base_ Right_ Dorsal			**Major_ Right_ Dorsal**	
Thumb	DenseNet201	85.26	Thumb	DenseNet201	84.21
Index	DenseNet201	81.57	Index	DenseNet201	83.15
Middle	MobileNetV2	80.00	Ring	DenseNet201	83.68
Ring	MobileNetV2	80.00	Little	MobileNetV2	80.00
Little	DenseNet169	83.15			
	Minor_ Left_ Dorsal			**Fingernail_ Left_ Dorsal**	
Middle	DenseNet201	86.77	Thumb	DenseNet169	87.83
Ring	DenseNet201	99.47	Middle	DenseNet201	100
	Minor_ Right_ Dorsal		Ring	DenseNet201	99.47
Index	MobileNetV2	80.00		**Fingernail_ Right_ Dorsal**	
Middle	ResNet50V2	85.18	Index	Mobile Net	90.00
Ring	DenseNet169	83.15	Middle	Mobile Net	91.05
Little	MobileNetV2	80.00	Ring	Mobile Net	93.68

Table 8: Rank-1 recognition rate for the 11k Hands (left dorsal & right dorsal) & PolyUHD (right dorsal) datasets

	11KHands				**PolyUHD**	
	Left_ Dorsal		**Right_ Dorsal**		**Right_ Dorsal**	
	DenseNet201	**InceptionV3**	**DenseNet201**	**InceptionV3**	**DenseNet201**	**InceptionV3**
Dis.	Base_ Left_ Dorsal_ Index (Rank-1)		Base_ Right_ Dorsal_ Index (Rank-1)		Base_ Right_ Dorsal_ Index (Rank-1)	
HamD	76.41	83.30	71.60	73.66	76.35	80.58
JaD	99.64	99.89	93.38	94.55	87.72	91.55
BB	97.28	99.25	89.94	90.54	91.72	89.48
BC	99.50	100	95.05	96.62	98	100
Dis.	Base_ Left_ Dorsal_ Little (Rank-1)		Base_ Right_ Dorsal_ Little (Rank-1)		Base_ Right_ Dorsal_ Little (Rank-1)	
HamD	79.17	91.31	70.74	79.69	74.47	77.66
JaD	87.68	99.72	92.30	94.46	82.36	86.21
BB	93.53	97.70	81.53	93.98	85.36	94.48
BC	94.49	99.78	87.45	92.72	89.76	98.72
Dis.	Base_ Left_ Dorsal_ Middle (Rank-1)		Base_ Right_ Dorsal_ Middle (Rank-1)		Base_ Right_ Dorsal_ Middle (Rank-1)	
HamD	78.25	83.063	73.65	75.28	76.56	80.26
JaD	78.18	98.63	93.55	89.35	77.91	88.39
BB	82.54	92.18	83.24	90.16	80.88	90.87
BC	100	100	93.82	94.01	90.27	97.06
Dis.	Base_ Left_ Dorsal_ Ring (Rank-1)		Base_ Right_ Dorsal_ Ring (Rank-1)		Base_ Right_ Dorsal_ Ring (Rank-1)	
HamD	77.95	84.97	71.28	75.22	80.6	82.1
JaD	83.26	88.65	85.23	87.63	86.12	87.52
BB	99.17	99.65	91.31	92	95.65	97.05
BC	99.87	100	89.29	92.60	97.05	98.85

Table 8: Continued

	11KHands				PolyUHD	
	Left_ Dorsal		Right_ Dorsal		Right_ Dorsal	
	DenseNet201	InceptionV3	DenseNet201	InceptionV3	DenseNet201	InceptionV3
Dis.	Base_ Left_ Dorsal_ Thumb (Rank-1)		Base_ Right_ Dorsal_ Thumb (Rank-1)		Base_ Right_ Dorsal_ Thumb (Rank-1)	
HamD	85.92	88.30	70.05	82.33	77.84	80.29
JaD	87.87	90.15	86.51	89.47	80.18	86.54
BB	99.41	99.51	86.37	87.10	84.91	89.89
BC	98.25	100	94.49	94.73	89.69	90.66
Dis.	Fingernail _Left_ Dorsal_ Index (Rank-1)		Fingernail _Right _ Dorsal_ Index (Rank-1)		Fingernail_ Right_ Dorsal_ Index (Rank-1)	
HamD	77.61	86.61	72.96	81.21	70.78	80.6
JaD	98.85	92.26	89.83	91.96	85.81	90.02
BB	99.39	99.96	88.70	90.78	87.29	89.30
BC	100	100	98.18	99.65	95.06	93.88
Dis.	Fingernail _ Left_ Dorsal_ Little (Rank-1)		Fingernail _ Right_ Dorsal_ Little (Rank-1)		Fingernail_ Right_ Dorsal_ Little (Rank-1)	
HamD	78.32	86.98	72	83.09	71.50	80.21
JaD	98.75	99	91.17	93.37	90.30	92.58
BB	99.38	99.72	90.09	95.45	90.08	93.32
BC	99.99	100	98.76	100	92.04	95.68
Dis.	Fingernail _ Left_ Dorsal_ Middle (Rank-1)		Fingernail _ Right_ Dorsal_ Middle (Rank-1)		Fingernail_ Right_ Dorsal_ Middle (Rank-1)	
HamD	85.71	89.63	80.22	85.57	75.17	80.09
JaD	93.35	100	94.41	96.04	90.96	93.87
BB	100	100	81.73	92.21	90.70	91.93
BC	100	100	96.37	99.47	100	100
Dis.	Fingernail_ Left_ Dorsal_ Ring (Rank-1)		Fingernail _ Right_ Dorsal_ Ring (Rank-1)		Fingernail_ Right_ Dorsal_ Ring (Rank-1)	
HamD	72.38	83.69	71.74	80.80	70.70	79.12
JaD	100	100	93.11	95.29	92.94	94.58
BB	100	100	83.64	95.38	80.49	89.10
BC	100	100	98.27	99.03	98.67	100
Dis.	Fingernail _ Left_ Dorsal_ Thumb (Rank-1)		Fingernail _ Right_ Dorsal_ Thumb (Rank-1)		Fingernail_ Right_ Dorsal_ Thumb (Rank-1)	
HamD	70.50	82.33	70.07	72.28	71.59	79.57
JaD	99.69	99.67	93.51	89.47	95.41	97.97
BB	99.46	99.86	86.37	87.10	87.08	90.09
BC	99.74	99.81	100	100	100	100
Dis.	Major_ Left_ Dorsal_ Index (Rank-1)		Major_ Right_ Dorsal_ Index (Rank-1)		Major_ Right_ Dorsal_ Index (Rank-1)	
HamD	77.94	79.20	71.68	73.47	72.47	74.23
JaD	99.26	99.68	90.38	94.69	94.01	97.00
BB	99.76	99.81	82.95	91.47	93.30	96.50
BC	99.68	100	93.27	95.33	95.70	99.90
Dis.	Major_ Left_ Dorsal_ Little (Rank-1)		Major_ Right_ Dorsal_ Little (Rank-1)		Major_ Right_ Dorsal_ Little (Rank-1)	
HamD	75.56	77.1	71.57	74.74	78.39	80.02
JaD	99.50	99.75	92.96	94.52	99.78	99.89
BB	99.72	99.86	80.41	94.67	99.89	100
BC	87.70	99.88	91.78	98.60	95.49	98.27
Dis.	Major_ Left_ Dorsal_ Middle (Rank-1)		Major_ Right_ Dorsal_ Middle (Rank-1)		Major_ Right_ Dorsal_ Middle (Rank-1)	
HamD	73.54	83.77	71.44	80.95	70.51	79.26
JaD	99.36	99.66	94.35	96.63	89.83	93.98
BB	99.72	99.79	81.01	95.41	97.53	97.89
BC	99.80	99.86	94.60	99.34	98.70	95.68

Table 8: Continued

	11KHands				PolyUHD	
	Left_ Dorsal		Right_ Dorsal		Right_ Dorsal	
	DenseNet201	InceptionV3	DenseNet201	InceptionV3	DenseNet201	InceptionV3
Dis.	Major_ Left_ Dorsal_ Ring (Rank-1)		Major_ Right_ Dorsal_ Ring (Rank-1)		Major_ Right_ Dorsal_ Ring (Rank-1)	
HamD	76.56	79.24	80.90	86.57	77.24	81.93
JaD	95.51	97.69	99.72	99.17	93.83	95.60
BB	86.74	90.84	99.89	99.21	90.52	96.90
BC	100	100	99.70	99.35	100	100
Dis.	Major_ Left_ Dorsal_ Thumb (Rank-1)		Major_ Right_ Dorsal_ Thumb (Rank-1)		Major_ Right_ Dorsal_ Thumb (Rank-1)	
HamD	73.53	76.72	73.18	76.94	71.91	74.08
JaD	97.05	97.60	93.61	95.58	89.37	92.94
BB	96.57	98.80	86.89	86.85	82.91	84.28
BC	100	100	91.95	96.45	100	100
Dis.	Minor_ Left_ Dorsal_ Index (Rank-1)		Minor_ Right_ Dorsal_ Index (Rank-1)		Minor_ Right_ Dorsal_ Index (Rank-1)	
HamD	73.91	74.48	71.89	73.70	71.28	72.41
JaD	96.51	94.22	92.22	93.95	90.06	91.00
BB	85.93	96.43	83.58	95.35	90.71	93.68
BC	93.26	100	89.36	92.97	88.35	94.29
Dis.	Minor_ Left_ Dorsal_ Little (Rank-1)		Minor_ Right_ Dorsal_ Little (Rank-1)		Minor_ Right_ Dorsal_ Little (Rank-1)	
HamD	79.52	81.03	73.45	78.85	70.17	78.25
JaD	91.51	95.86	89.63	93.07	85.97	89.96
BB	95.76	96.66	90.62	94.61	86.30	87.89
BC	92.47	100	90.52	97.71	89.09	93.67
Dis.	Minor_ Left_ Dorsal_ Middle (Rank-1)		Minor_ Right_ Dorsal_ Middle (Rank-1)		Minor_ Right_ Dorsal_ Middle (Rank-1)	
HamD	78.54	83.77	76.94	80.32	73.51	77.22
JaD	90.09	92.71	85.72	89.36	83.03	86.98
BB	86.99	92.84	84.20	90.16	81.70	87.68
BC	98	100	90.58	90.81	93.49	94.07
Dis.	Minor_ Left_ Dorsal_ Ring (Rank-1)		Minor_ Right_ Dorsal_ Ring (Rank-1)		Minor_ Right_ Dorsal_ Ring (Rank-1)	
HamD	79.08	84.74	77.68	83.70	76.66	81.47
JaD	90.39	95.34	86.53	94.62	81.81	90.18
BB	92.57	93.27	86.09	88.29	85.89	87.08
BC	99.93	100	87.54	91.98	90.51	93.69
Dis.	All_Left_Dorsal_11K		All_Right_Dorsal_11K		All_ Right_ Dorsal_ PolyUHD	
HamD	**77.38**	**83.17**	**73.31**	**78.86**	**74.08**	**78.91**
JaD	**94.02**	**96.86**	**91.48**	**93.32**	**88.28**	**91.93**
BB	**95.46**	**97.69**	**86.24**	**92.14**	**88.57**	**91.96**
BC	**98.11**	**99.96**	**93.42**	**96.28**	**94.83**	**97.07**

5.0 DISCUSSION

This section discusses the results obtained by the multimodal deep learning proposed for multi-biometrics of the dorsal finger knuckle and fingernails, with the datasets used and similarity distances for the rank-1 recognition accuracy. Using multimodal deep learning for personal identification recognition, through the experiments we conducted that it is the best model of DenseNet201 and Inception V3 models, regardless of fine-tuning models. After adding fine-tuning to both inception V3 models and denseNet201 model, we observed much better and more distinct performance, with the Inception V3 model performing better than the denseNet201 model in extracting abstract and high-level features on both the 11k left and right dorsal hands dataset and PolyUHD right dorsal hands in tables (3,4,5,6) in section (4.2), where the F1_score is 87.83% for denseNet201 model_ 11k Hands (left dorsal), 92.94% for denseNet201 model_ 11k Hands (Right dorsal) and 93.51% for denseNet201 model _ PolyU HD (right dorsal), whereas the F1_score is 95.39% for inception V3 model_ 11k Hands (left dorsal), 91.84% for inception

V3 Model_ 11k Hands (right dorsal) and 95.59% for inception V3 model _ PolyU HD (right dorsal) because there are many benefits to denseNet201 model requires less parameters and processing time, and automatically scales to hundreds of layers, without causing any optimization problems. Compared to the Inception V3 model is the most accurate and efficient model for processing input images. It is continuously being enhanced and has increased efficiency in identifying particular patterns, features, and images.

In the matching process, we obtained the results of similarity distances (Hamming Distance (HamD), Jaccard Distance (JaD), Braun-Blanquet Distance (BB), and Bray-Curtis Distance (BC)) to obtain the rank-1 recognition accuracy both for the 11k Hands and PolyUHD datasets. These metrics effectively capture differences or overlaps between binary or numerical data, enabling accurate matching and classification. Their use enhances the robustness of biometric identification by offering varied perspectives on similarity, improving overall recognition performance. We achieved the highest results for both hands in almost all fingernails in both the inception V3 model and DenseNet201, and then achieved the highest results in base, major and minor in the Inception V3 model compared to the DenseNet201 model. The lowest results were achieved in the minor denseNet201 model. In Table 8, we can observe that the proposed approach obtained the rank-1 accuracy for the 11k Hands (left dorsal) dataset for both the Inception V3 model and the DenseNet201 model. The fingernail rank-1 accuracies were 100% in the little finger,100% in the index, middle and ring fingers and 99.81%,99.74% in the thumb fingers for the inception V3 model and the denseNet201 model_ 11k Hands (left dorsal). The base obtained a rank-1 accuracy of 100% in the middle finger for the inception V3 model_ 11k Hands (left dorsal) and 100% in the index, ring and thumb fingers for the inception V3 model and denseNet201 model_ 11k Hands (left dorsal). The major obtained a rank-1 accuracy of 100% in the ring, index and thumb fingers and 99.88%, 99.86% in the little and middle fingers for the inception V3 model_ 11k Hands (left dorsal). Overall, we can show the minor obtained a rank-1 accuracy of 100% in the little, index, middle and ring fingers for Inception V3 model_ 11k Hands (left dorsal), 99.93% for DenseNet201 model_ 11k Hands (left dorsal) in the ring for denseNet201 model_ 11k Hands (left dorsal). We can observe that the proposed approach obtained the rank-1 accuracy for the 11k Hands (right dorsal) dataset for both the Inception V3 model and the DenseNet201 model.

The fingernail rank-1 accuracies were 100% in the little finger for the inception V3 model_ 11k Hands (right dorsal), 100% in the thumb fingers for the inception V3 model and the DenseNet201 model_ 11k Hands (right dorsal). The base rank-1 accuracies are 96.62% in the index for the Inception V3 model_ 11k Hands (right dorsal). The major rank-1 accuracies were 99.70%,99.35% in the thumb fingers for the inception V3 model and the denseNet201 model_ 11k Hands (right dorsal). Overall, we can show that the minor knuckles obtained a rank-1 accuracy of 97.71% in the little finger for the Inception V3 model 11k Hands (right dorsal). We can observe that the proposed approach obtained the rank-1 accuracy for the PolyUHD (right dorsal) dataset for both the Inception V3 and the DenseNet201 models. The fingernail rank-1 accuracies were 100%, 98.68%, 97.97% and 95.68% in the ring, little and thumb fingers for the inception V3 model _ PolyUHD (right dorsal), 100% in the middle and thumb fingers right dorsal hand for the inception V3 model and denseNet201 _ PolyUHD (right dorsal). The base achieved a rank-1 accuracy of 100% and 98.72% in the index and little fingers for inception V3 model_ PolyUHD (right dorsal), 98% in the index fingers for denseNet201 model_ PolyUHD (right dorsal) and 97.06%, 97.05% and 98.85% in the ring and middle finger for inception V3 model_ PolyUHD (right dorsal). The major rank-1 accuracies were 100%, 99.90% and 95.70% in the ring, index and thumb fingers for inception V3 model and denseNet201 model_ PolyUHD (right dorsal), 100% in the ring and little fingers for inception V3 model_ PolyUHD (right dorsal), Overall, we can show that the minor knuckles obtained a rank-1 accuracy of 94.29% in the index finger for inception V3 model _ PolyUHD (right dorsal). Finally, we obtained the highest results in all key components for the hand in the Inception V3 model for 11k Hands (left dorsal) and PolyUHD (right dorsal). we can observe that the proposed approach obtained the all hands rank-1 accuracies were 99.96% and 98.11% for inception V3 model and denseNet201 model _11k Hands (left dorsal), 96.28% and 93.42% for inception V3 model and denseNet201 model _11k Hands (right dorsal) and 97.07% and 94.83% for inception V3 model and denseNet201 model _ PolyUHD (right dorsal). Fig. 14 illustrates the rank_1 recognition of the finger knuckle patterns and fingernails of the left and right hands in the 11k Hands & right hands in the PolyUHD, additional comparison between the rank_1 recognition for denseNet201 & inception V3 Models.

Interestingly, the best-performing base models in terms of rank-1 recognition accuracy, from highest to lowest, are Inception V3, DenseNet201, FKPIndexNet [66], Deep CNN [67], ResNet50 [68], VGG16 [69], VGG19-F6[19], DenseNet [68], and ResNet34 [67]. Fig. 15 demonstrates the most basic (pre-trained) models that perform well in various sub-images for $(FKP \ \& \ FN)^{+}$.

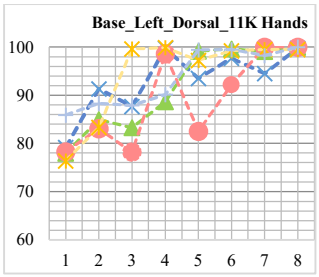
Base_Left_Dorsal_11K Hands
100
90
80
70
60
1 2 3 4 5 6 7 8

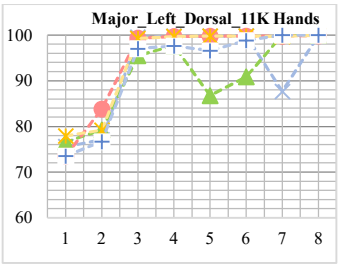
Major_Left_Dorsal_11K Hands
100
90
80
70
60
1 2 3 4 5 6 7 8

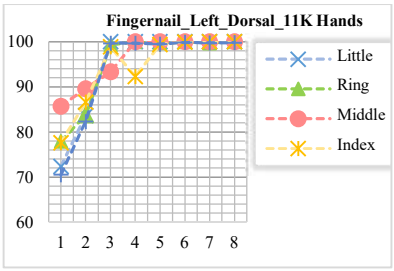
Fingernail_Left_Dorsal_11K Hands
100
90
80
70
60
1 2 3 4 5 6 7 8
Little
Ring
Middle
Index

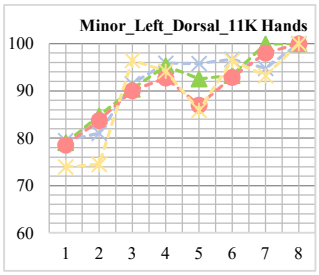
Minor_Left_Dorsal_11K Hands
100
90
80
70
60
1 2 3 4 5 6 7 8

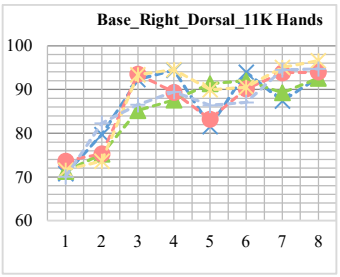
Base_Right_Dorsal_11K Hands
100
90
80
70
60
1 2 3 4 5 6 7 8

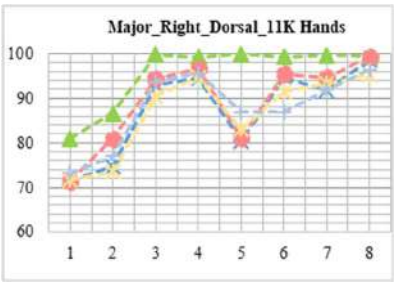
Major_Right_Dorsal_11K Hands
100
90
80
70
60
1 2 3 4 5 6 7 8

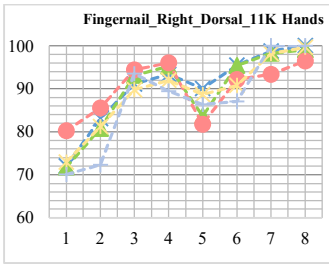
Fingernail_Right_Dorsal_11K Hands
100
90
80
70
60
1 2 3 4 5 6 7 8

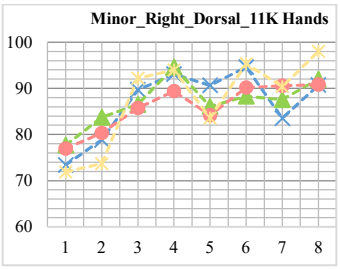
Minor_Right_Dorsal_11K Hands
100
90
80
70
60
1 2 3 4 5 6 7 8

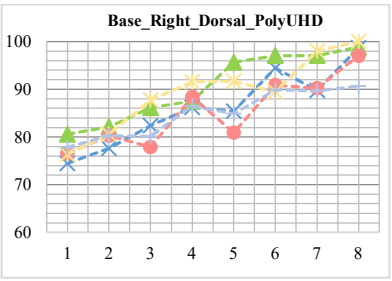
Base_Right_Dorsal_PolyUHD
100
90
80
70
60
1 2 3 4 5 6 7 8

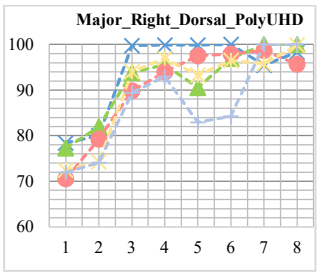
Major_Right_Dorsal_PolyUHD
100
90
80
70
60
1 2 3 4 5 6 7 8

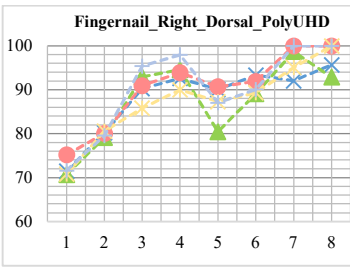
Fingernail_Right_Dorsal_PolyUHD
100
90
80
70
60
1 2 3 4 5 6 7 8

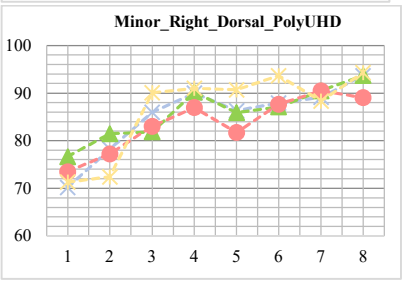
Minor_Right_Dorsal_PolyUHD
100
90
80
70
60
1 2 3 4 5 6 7 8

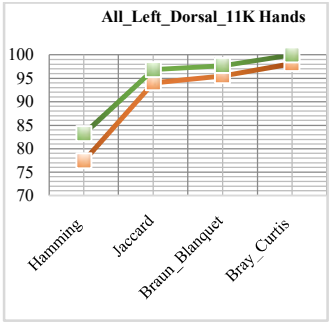
All_Left_Dorsal_11K Hands
100
95
90
85
80
75
70
Hamming
Jaccard
Braun_Blanquet
Bray_Curtis

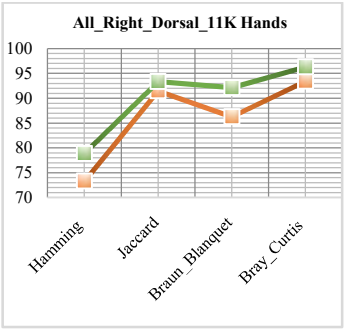
All_Right_Dorsal_11K Hands
100
95
90
85
80
75
70
Hamming
Jaccard
Braun_Blanquet
Bray_Curtis

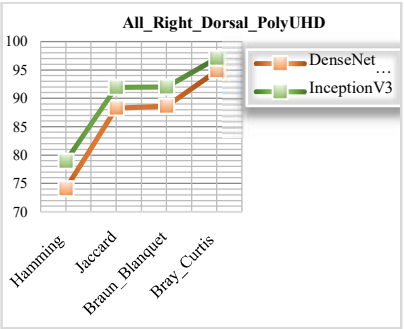
All_Right_Dorsal_PolyUHD
100
95
90
85
80
75
70
Hamming
Jaccard
Braun_Blanquet
Bray_Curtis
DenseNet
InceptionV3

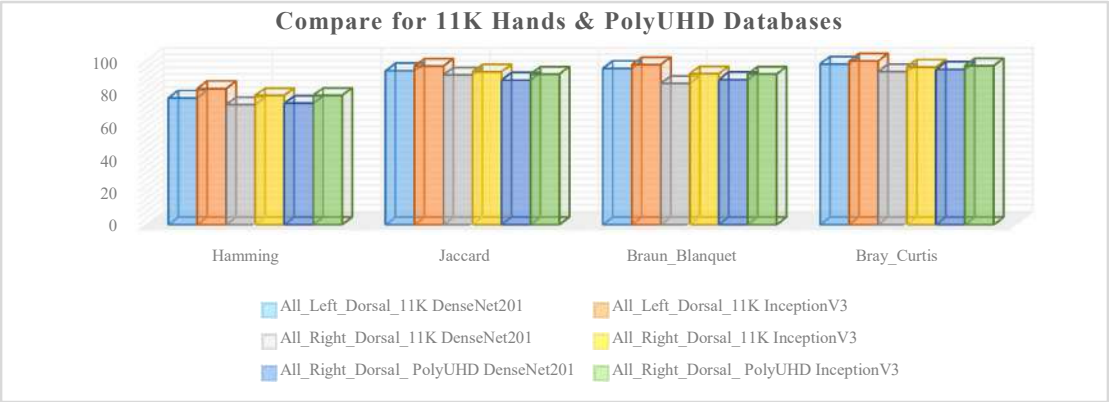

Fig. 14: The rank_1 for the proposed (FKP & FN)$^{+}$ and compare between the rank_1 recognition for DenseNet201 & InceptionV3 models for left and right hands in the 11kHands & Right Hands in the PolyUHD

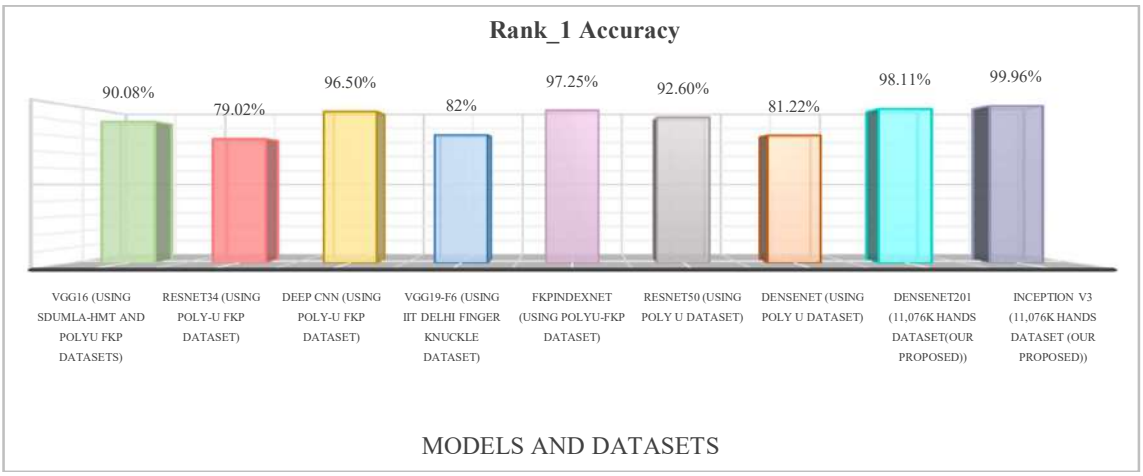

Fig. 15: Shows the rank-1 accuracy for all models with datasets for (FKP & FN)$^{+}$.

6.0 CONCLUSION AND FUTURE SCOPE

This research paper attempted to devise a novel structure of personal identification based on the recognition of finger knuckle patterns and fingernails (FKP & FN)$^{+}$. The proposed structure uses the dorsal surface of the five human hand components (fingernails (5), base knuckles (5), major knuckle (4), minor knuckle (4), and major knuckle of the thumb (1)). The proposed (FKP & FN)$^{+}$ approach uses all 19 hand components from two widely used datasets: 'PolyUHD' and the 11k Hands datasets. We are using the multi-model deep learning, fine-tune segmented subsets per component of the DenseNet201 model and fine-tune the Inception V3 model to extract abstract features. According to the multi-model deep learning-based approach proposed in the work, the patterns of the dorsal finger knuckle and fingernails play an important role in person recognition. The experimental results show its effectiveness, resilience, and dependability, due to the use of multi-model deep learning based on the fine-tuning of DenseNet201 and Inception V3 models. Low computational cost can be achieved using DenseNet201 and Inception V3. Moreover, compared to previous models that were already in use, the proposed approach produced the best results. The (FKP & FN)$^{+}$ suffers from limitations in some of the key point components (basic and Minor) due to its application to specific finger types (Little, Ring, Middle, Index, and Thumb) for both hands, where the parameter value was chosen inappropriately for the DenseNet201 and Inception V3. These limitations are a subject of future research using various feature extraction models, including MobileNet and ResNet50 models. In addition, as multimodal biometric systems have proven vulnerable to spoofing attempts, it will review them to strengthen its defenses against such attacks.

Authors' Declaration

- Conflicts of Interest: None.
- We hereby confirm that all the Figures and Tables in the manuscript are ours. Furthermore, any Figures and images that are not ours have been included with the necessary permission for re-publication, which is attached to the manuscript.

Authors' Contribution Statement

H.S.C., and T.A. participated in proposing the research idea, the significant roles that each researcher played can be summed up as follows: The author H.S.C. find relevant sources, collected the dataset and configured the final folders of each category, and designed the multimodal, including the architecture of the deep learning for each models, make descriptive tables, and analyze the results and tables. On the other hand, researcher T.A. played a major role in drawing the figures, writing algorithms, the grammatical aspect, the linguistic aspect, determining the scientific methodology of the research, determining the initial research directions, and directly supervising the intellectual and scientific material of the article.

REFERENCES

[1] A. Attia, Z. Akhtar, N. E. Chalabi, S. Maza, and Y. Chahir, "Deep rule-based classifier for finger knuckle pattern recognition system", *Evolving Systems,* vol. 12, no. 4, pp. 1015-1029, Dec. 2021. https://doi.org/10.1007/s12530-020-09359-w

[2] K. Usha and M. Ezhilarasan, "Finger knuckle biometrics–A review", *Computers & Electrical Engineering*, vol. 45, pp. 249-259, July. 2015. https://doi.org/10.1016/j.compeleceng.2014.11.008

[3] M. Anbari and A. M. Fotouhi, "Finger knuckle print recognition for personal authentication based on relaxed local ternary pattern in an effective learning framework", *Machine Vision and Applications*, vol. 32, no. 3, pp. 55, March. 2021. https://doi.org/10.1007/s00138-021-01178-6

[4] C. R. Daniel III, B. M. Piraccini, and A. Tosti, "The nail and hair in forensic science", *Journal of the American Academy of Dermatology,* vol. 50, no. 2, pp. 258-261, Feb. 2004. https://doi.org/10.1016/j.jaad.2003.06.008

[5] K. H. Cheng and A. Kumar, "Efficient and accurate 3D finger knuckle matching using surface key points", *IEEE Transactions on Image Processing,* vol. 29, pp. 8903-8915, Sep. 2020. https://doi.org/10.1109/tip.2020.3021294

[6] M. Y. Shakor and N. M. S. Surameery, "CNN-Based Transfer Learning for 3D Knuckle Recognition", *Advances in Multimedia,* vol. 2023, no. 1, pp. 6147422, Feb. 2023. https://doi.org/10.1155/2023/6147422

[7] A. Zohrevand, Z. Imani, and M. Ezoji, "Deep convolutional neural network for finger-knuckle-print recognition", *International Journal of Engineering,* vol. 34, no. 7, pp. 1684-1693, Jul. 2021. https://doi.org/10.5829/ije.2021.34.07a.12

[8] S. Daas, A. Yahi, T. Bakir, M. Sedhane, M. Boughazi, and E. B. Bourennane, "Multimodal biometric recognition systems using deep learning based on the finger vein and finger knuckle print fusion", *IET Image Processing,* vol. 14, no. 15, pp. 3859-3868, Feb. 2020. https://doi.org/10.1049/iet-ipr.2020.0491

[9] M. Oudah, A. Al-Naji, and J. Chahl, "Hand gesture recognition based on computer vision: a review of techniques", *Journal of Imaging,* vol. 6, no. 8, pp. 73, July. 2020. https://doi.org/10.3390/jimaging6080073

[10] A. Kamboj, R. Rani, A. Nigam, and R. R. Jha, "CED-Net: context-aware ear detection network for unconstrained images", *Pattern Analysis and Applications,* vol. 24, no. 2, pp. 779-800, Nov. 2021. https://doi.org/10.1007/s10044-020-00914-4

[11] F. Juefei-Xu, E. Verma, and M. Savvides, "DeepGender2: A generative approach toward occlusion and low-resolution robust facial gender classification via progressively trained attention shift convolutional neural networks (PTAS-CNN) and deep convolutional generative adversarial networks (DCGAN)". *Deep Learning for Biometrics: Springer,* Aug. 2017, pp. 183-218. https://doi.org/10.1007/978-3-319-61657-58

[12] R. S. Kuzu, E. Piciucco, E. Maiorana, and P. Campisi, "On-the-fly finger-vein-based biometric recognition using deep neural networks".*IEEE Transactions on Information Forensics and Security,* Vol. 15, Feb. 2020, pp. 2641-2654. https://doi.org/10.1109/tifs.2020.2971144

[13] X. Di and V. M. Patel, "Deep learning for tattoo recognition". *Deep Learning for Biometrics: Springer*, August. 2017,pp. 241-256. https://doi.org/10.1007/978-3-319-61657-510

[14] S. Bhattacharya *et al.*, "Deep learning and medical image processing for coronavirus (COVID-19) pandemic: A survey", *Sustainable cities and society,* vol. 65, pp. 102589, Feb. 2021. https://doi.org/10.1016/j.scs.2020.102589

[15] M. Chaa, Z. Akhtar, and A. Attia, "3D palmprint recognition using unsupervised convolutional deep learning network and SVM classifier", *IET Image Processing,* vol. 13, no. 5, pp. 736-745, Mar. 2019. https://doi. 10.1049/iet-ipr.2018.5642

[16] G. Jaswal, A. Nigam, and R. Nath, "Finger knuckle image based personal authentication using DeepMatching", in *2017 IEEE International Conference on Identity, Security and Behavior Analysis (ISBA*), 22-24 Feb. 2017, pp. 1-8: IEEE. https://doi.org/10.1109/isba.2017.7947706

[17] M. Diarra, A. K. Jean, B. A. Bakary, and K. B. Médard, "Study of deep learning methods for fingerprint recognition", *International Journal of Recent Technology and Engineering (IJRTE),* vol. 10, no. 3, pp. 192-197, Sep. 2021. https://doi. org/ 10.35940/ijrte.C6478.0910321

[18] A. S. Tarawneh *et al.*, "Deepknuckle: Deep learning for finger knuckle print recognition", *Electronics,* vol. 11, no. 4, pp. 513, February. 2022. https://doi.org/10.3390/electronics11040513

[19] R. Chlaoua, A. Meraoumia, K. E. Aiadi, and M. Korichi, "Deep learning for finger-knuckle-print identification system based on PCANet and SVM classifier", *Evolving Systems,* vol. 10, no. 2, pp. 261-272, Jun. 2019. https://doi.org/10.1007/s12530-018-9227-y

[20] L. Zhang, L. Zhang, D. Zhang, and H. Zhu, "Ensemble of local and global information for finger–knuckle-print recognition", *Pattern recognition,* vol. 44, no. 9, pp. 1990-1998, Sep. 2011. https://doi.org/10.1016/j.patcog.2010.06.007

[21] K. Usha and M. Ezhilarasan, "Personal recognition using finger knuckle shape oriented features and texture analysis", *Journal of King Saud University-Computer and Information Sciences,* vol. 28, no. 4, pp. 416-431, Oct. 2016. http://doi.org/10.1016/j.jksuci.2015.02.004

[22] J. Joshi, S. Nangia, K. Tiwari, and K. Gupta, "Finger Knuckleprint based personal authentication using siamese network", in *2019 6th international conference on signal processing and integrated networks (SPIN)*, 07-08 Mar. 2019, pp. 282-286: IEEE. https://doi.org/10.1109/spin.2019.8711663

[23] M. A. Sadik, M. N. Al-Berry, and M. Roushdy, "A survey on the finger knuckle prints biometrie", in *2017 Eighth International Conference on Intelligent Computing and Information Systems (ICICIS)*, 05-07 December 2017, pp. 197-204: IEEE. https://doi.org/10.1109/intelcis.2017.8260036

[24] Z. S. Shariatmadar and K. Faez, "A novel approach for Finger-Knuckle-Print recognition based on Gabor feature fusion", in *2011 4th International Congress on Image and Signal Processing*, 15-17 Oct. 2011, vol. 3, pp. 1480-1484: IEEE. https://doi.org/10.1109/cisp.2011.6100450

[25] A. Kumar and Z. Xu, "Personal identification using minor knuckle patterns from palm dorsal surface", *IEEE Transactions on Information Forensics and Security,* vol. 11, no. 10, pp. 2338-2348, May. 2016. https://doi.org/10.1109/tifs.2016.2574309

[26] M. Amina, "Efficient person identification by Finger-Knuckle-Print based on Discrete Cosine Transform Network", University Kasdi Merbah-Ouargla, June 2018.

[27] L. Zhang, L. Zhang, and D. Zhang, "Finger-knuckle-print: a new biometric identifier", in *2009 16th IEEE international conference on image processing (ICIP)*, 07-10 Nov. 2009, pp. 1981-1984: IEEE. https://doi.org/10.1109/icip.2009.5413734

[28] A. Attia, A. Moussaoui, M. Chaa, and Y. Chahir, "Finger-knuckle-print recognition system based on features-level fusion of real and imaginary images", *Journal on Image and Video Processing,* vol.08, iss. 04, 2018. https://doi.org/10.21917/ijivp.2018.0252

[29] N. E. Chalabi, A. Attia, and A. Bouziane, "Multimodal finger dorsal knuckle major and minor print recognition system based on PCANET deep learning", *ICTACT J Image Video Process,* vol. 10, no. 3, pp. 2153-2158, February. 2020. https://doi.org/10.21917/ijivp.2020.0308

[30] M. Afifi, "11K Hands: Gender recognition and biometric identification using a large dataset of hand images", *Multimedia Tools and Applications,* vol. 78, pp. 20835-20854, Mar. 2019. https://doi.org/10.1007/s11042-019-7424-8

[31] F. Zhuang *et al.*, "A comprehensive survey on transfer learning", in *Proceedings of the IEEE,* vol. 109, no. 1, 2020, pp. 43-76. https://doi.org/10.1109/JPROC.2020.3004555

[32] R. Ribani and M. Marengoni, "A survey of transfer learning for convolutional neural networks", in *2019 32nd SIBGRAPI conference on graphics, patterns and images tutorials (SIBGRAPI-T)*, 28-31 Oct. 2019, pp. 47-57: IEEE. https://doi.org/10.1109/sibgrapi-t.2019.00010

[33] G. Huang, Z. Liu, L. Van Der Maaten, and K. Q. Weinberger, "Densely connected convolutional networks", in *Proceedings of the IEEE conference on computer vision and pattern recognition*, 2017, pp. 4700-4708. https://doi.org/10.1109/cvpr.2017.243

[34] C. Szegedy *et al.*, "Going deeper with convolutions", in *Proceedings of the IEEE conference on computer vision and pattern recognition*, 2015, pp. 1-9. https://doi.org/10.1109/CVPR.2015.7298594

[35] C. Szegedy, V. Vanhoucke, S. Ioffe, J. Shlens, and Z. Wojna, "Rethinking the inception architecture for computer vision", in *Proceedings of the IEEE conference on computer vision and pattern recognition*, 2016, pp. 2818-2826. https://doi.org/10.1109/CVPR.2016.308

[36] R. Yan and L. Shao, "Blind image blur estimation via deep learning", *IEEE Transactions on Image Processing,* vol. 25, no. 4, pp. 1910-1921, Feb. 2016. https://doi.org/10.1109/TIP.2016.2535273

[37] H. Yamaura, M. Tamura, and S. Nakamura, "Image blurring method for enhancing digital content viewing experience," in *International Conference on Human-Computer Interaction*, 01 Jun. 2018: Springer, pp. 355-370. https://doi.org/10.1007/978-3-319-91238-729

[38] V. Chernov, J. Alander, and V. Bochko, "Integer-based accurate conversion between RGB and HSV color spaces", *Computers & Electrical Engineering,* vol. 46, pp. 328-337, Aug. 2015. https://doi.org/10.1016/j.compeleceng.2015.08.005

[39] D. J. Bora, A. K. Gupta, and F. A. Khan, "Comparing the performance of L* A* B* and HSV color spaces with respect to color image segmentation", *International Journal of Emerging Technology and Advanced Engineering,* vol. 5, Iss. 2, Jun. 2015, arXiv preprint arXiv:1506.01472.

[40] F. S. Hassan and A. Gutub, "Improving data hiding within colour images using hue component of HSV colour space", *CAAI Transactions on Intelligence Technology,* vol. 7, no. 1, pp. 56-68, Mar. 2022. https://doi.org/10.1049/cit2.12053

[41] K. A. M. Said and A. B. Jambek, "Analysis of image processing using morphological erosion and dilation", in *Journal of Physics: Conference Series*, vol. 2071, no. 1, p. 012033: IOP Publishing, Oct. 2021. https://doi.org/10.1088/1742-6596/2071/1/012033

[42] S. Raju and E. Rajan, "Skin Texture Analysis Using Morphological Dilation and Erosion", *Int. J. Pure Appl. Math,* vol. 118, pp. 205-223, 2018.

[43] J. E. Rodríguez and D. Ayala, "Erosion and Dilation on 2-D and 3-D Digital Images: A New Size-Independent Approach", in *VMV*, 2001.

[44] B. Justusson, "Median filtering: Statistical properties", *Two-dimensional digital signal prcessing II: transforms and median filters*, Jan. 2006, pp. 161-196. https://doi.org/10.1007/bfb0057597

[45] H. Soni and D. Sankhe, “Image restoration using adaptive median filtering”, *International Research Journal of Engineering and Technology (IRJET),* vol. 6, no. 10, Oct. 2019.

[46] K. O. Boateng, B. W. Asubam, and D. S. Laar, “Improving the effectiveness of the median filter”, *International Journal of Electronics and Communication Engineering,* vol.5, no.1, pp. 85-97, 2012.

[47] R. Kumar, A. Bajpai, and A. Sinha, “Mediapipe and CNNs for real-time asl gesture recognition”, *arXiv preprint arXiv:2305.05296,* May 2023.

[48] G. Amprimo, G. Masi, G. Pettiti, G. Olmo, L. Priano, and C. Ferraris, “Hand tracking for clinical applications: validation of the Google MediaPipe Hand (GMH) and the depth-enhanced GMH-D frameworks”, *Biomedical Signal Processing and Control,* vol. 96, pp. 106508, Jun. 2024. https://doi.org/10.1016/j.bspc.2024.106508

[49] K. Usha and M. Ezhilarasan, “Fusion of geometric and texture features for finger knuckle surface recognition”, *Alexandria Engineering Journal,* vol. 55, no. 1, pp. 683-697, Nov. 2016. https://doi.org/10.1016/j.aej.2015.10.003

[50] S.-S. Choi, S.-H. Cha, and C. C. Tappert, "A survey of binary similarity and distance measures," *Journal of systemics, cybernetics and informatics,* vol. 8, no. 1, pp. 43-48, Jan. 2010.

[51] M. Muniswamaiah, T. Agerwala, and C. C. Tappert, "Applications of Binary Similarity and Distance Measures," *arXiv preprint arXiv:2307.00411,* 2023.

[52] R. Todeschini, V. Consonni, H. Xiang, J. Holliday, M. Buscema, and P. Willett, “Similarity coefficients for binary chemoinformatics data: overview and extended comparison using simulated and real data sets”, *Journal of chemical information and modeling,* vol. 52, no. 11, pp. 2884-2901, Oct. 2012. https://doi.org/10.1021/ci300261r

[53] M. Paradowski, “On the order equivalence relation of binary association measures”, *International Journal of Applied Mathematics and Computer Science,* vol. 25, no. 3, pp. 645-657, 2015. https://doi.org/ 10.1515/amcs-2015-0047

[54] Y. Sari, M. Alkaff, and R. A. Pramunendar, “Iris recognition based on distance similarity and PCA”, in *AIP Conference Proceedings*, 2018, vol. 1977, no. 1: AIP Publishing. https://doi.org/10.1063/1.5042900

[55] R. Shyam and Y. N. Singh, “Recognizing individuals from unconstrained facial images”, in *Intelligent Systems Technologies and Applications: vol. 1*: Springer, 2015, 29 Aug. 2015, pp. 383-392. https://doi.org/10.1007/978-3-319-23036-8_33

[56] D. M. Ibrahim, N. M. Elshennawy, and A. M. Sarhan, “Deep-chest: Multi-classification deep learning model for diagnosing COVID-19, pneumonia, and lung cancer chest diseases”, *Computers in biology and medicine,* vol. 132, p. 104348, Mar. 2021. https://doi.org/10.1016/j.compbiomed.2021.104348

[57] A. A. Nafea, N. Omar, and Z. M. Al-qfail, “Artificial neural network and latent semantic analysis for adverse drug reaction detection”, *Baghdad Science Journal,* vol. 21, no. 1, pp. 0226-0226, May.2024. https://doi.org/10.21123/bsj.2023.7988

[58] M. M. Mijwil and M. Aljanabi, “A comparative analysis of machine learning algorithms for classification of diabetes utilizing confusion matrix analysis”, *Baghdad Science Journal,* vol. 20, no. 10.21123, Oct. 2023. https://doi.org/10.21123/bsj.2023.9010

[59] N. Salih, M. Ksantini, N. Hussein, D. B. Halima, A. A. Razzaq, and S. Ahmed, “Deep learning models and fusion classification technique for accurate diagnosis of retinopathy of prematurity in preterm newborn”, *Baghdad Science Journal,* vol. 20, no.5, *Oct.* 2023. https://doi.org/10.21123/bsj.2023.8747

[60] N. Al Musalhi, A. M. Al Wahaibi, and M. Abbas, “Implementing Real-time Visitor Counter Using Surveillance Video and MobileNet-SSD Object Detection: The Best Practice”, *Baghdad Science Journal,* vol. 21, no. 5 (SI), pp. 1775-1775, May.2024. https://doi.org/10.21123/bsj.2024.10540

[61] R. Jopate, P. K. Pareek, and A. S. Z. J. Al Hasani, "Prediction of Thyroid Classes Using Feature Selection of AEHOA Based CNN Model for Healthy Lifestyle", *Baghdad Science Journal,* vol. 21, no. 5 (SI), pp. 1786-1786, May.2024. https://doi.org/10.21123/bsj.2024.10547

[62] Z. Ahanin, M. A. Ismail, and T. Herawan, "Performance Evaluation of Multilabel Emotion Classification Using Data Augmentation Techniques", *Malaysian Journal of Computer Science,* vol. 37, no. 2, pp. 155-170, Apr.2024. https://doi.org/10.22452/mjcs.vol37no2.4

[63] S. K. Hamed, M. J. Ab Aziz, and M. R. Yaakub, "Disinformation detection about islamic issues on social media using deep learning techniques", *Malaysian Journal of Computer Science,* vol. 36, no. 3, pp. 242-270, Jul.2023. https://doi.org/10.22452/mjcs.vol36no3.3

[64] A. Alomari, N. Idris, A. Qalid, and I. Alsmadi, "Improving Coverage and Novelty of Abstractive Text Summarization Using Transfer Learning and Divide and Conquer Approaches", *Malaysian Journal of Computer Science,* vol. 36, no. 3, pp. 271-288, Jul. 2023. https://doi.org/10.22452/mjcs.vol36no3.4

[65] S. C. Pravin and M. Palanivelan, "WDSAE-DNDT Based Speech Fluency Disorder Classification", *Malaysian Journal of Computer Science,* vol. 35, no. 3, pp. 222-242, Jul. 2022. https://doi.org/10.22452/mjcs.vol35no3.3

[66] G. Arora, A. Singh, A. Nigam, H. M. Pandey, and K. Tiwari, "FKPIndexNet: An Efficient Learning Framework for Finger-Knuckle-Print Database Indexing to Boost Identification", *Knowledge-Based Systems,* vol.239, pp.108028, Mar. 2022. https://doi.org/10.1016/j.knosys.2021.108028

[67] A. Zohrevand, Z. Imani, and M. Ezoji, "Deep Convolutional Neural Network for Finger-knuckle-print Recognition", International Journal of Engineering, vol. 34, no. 7, pp. 1684-1693, 2021. https://doi.org/10.5829/ije.2021.34.07a.12

[68] A. Altaheret *et al.*,"Finger Knuckle Print Classification Using Pretrained Vision Models", in 2023 IEEE 20th International Conference on Smart Communities: Improving Quality of Life using AI, Robotics and IoT (HONET), IEEE, Dec. 2023, pp. 62-67. https://doi.org/10.1109/honet59747.2023.10374940

[69] S. Daas, A. Yahi, T.Bakir, M. Sedhane, M. Boughazi, and E.B. Bourennane, "Multimodal biometric recognition systems using deep learning based on the finger vein and finger knuckle print fusion", IET Image Processing, vol. 14, Iss. 15, pp. 3859-3868, Dec. 2020. https://doi.org/10.1049/iet-ipr.2020.0491